We are thankful to the two referees for thoughtful comments which help improve the manuscript substantially. Following the reviewers' suggestions, we have revised the manuscript accordingly. Listed below are our point-by-point responses in blue to each comment that is repeated in italic.

Response to Referee #1

This paper reports an observational case study of pollution in Beijing around the APEC period, chiefly with an HR-AMS. The techniques used are fairly well-established, but the results presented are extremely interesting because this presented a unique opportunity to study the different sources of megacity pollution in isolation. Several interesting observations are made regarding the different sources of PMF-resolved organics and the changes in the oxidation state of the organics and the sizes of the particles. It is generally well written and very relevant to ACP, so I recommend publication after the comments below have been considered.

We thank the reviewer's positive comments.

This is not the only paper covering this case study; the paper Chen et al. (www.atmos-chem-phys-discuss.net/15/22889/2015/) also covers this from the perspective of the measurements made on the Beijing Meteorological Tower. While I have read both papers and I am satisfied that there is not too much overlap between the two papers, I find it strange that this paper makes no reference to the Chen et al. paper, especially as the two papers share the same corresponding author. It would be useful to discuss the relevance of the findings presented here in the context of the observations of the other paper.

Thanks the reviewer's comments. Chen et al. (2015) was now cited more in the revised manuscript for a better comparison with the results obtained at the ground site. For example, in section 3.1, we added "However, the measurements at 260 m at the same location showed significant decreases of 40–80% for all aerosol species during APEC, whereas the bulk aerosol composition was relatively similar before and during APEC as a result of synergetic controls of aerosol precursors over a regional scale(Chen et al., 2015). These results indicated the different sources of aerosol particles between the ground site and 260 m.".

General: The use of the term 'oxidative properties' seems a little odd. This is normally used to refer to the properties of oxidizing agents or their precursors (e.g. NO_x, O_3), but here it is the oxygen content of the organic aerosol that is under investigation. I think it would be more correct to refer to the 'oxidation properties' throughout the manuscript (as it is done in a few instances).

A good point. “oxidative properties” was changed to “oxidation properties” throughout the manuscript.

Page 23411, line 5: The statement that ‘the oxidative properties of aerosol particles remain largely unknown’ is a little odd because there have been a large number of papers focusing on this exact topic in the last seven years using the techniques used here. While it continues to be a subject of much interest, I don’t think the statement as it is written really stands.

Thank the reviewer’s comment. This sentence was now revised as “the oxidation properties of aerosol particles remain less understood”.

Page 23415: The terms ‘A-A’ and ‘I-A’ should be defined.

Thanks the reviewer’s comments. The AMS organic O/C tends to be biased low because of the influence of unimolecular ion decomposition reactions, in which a fragment with an electronegative atom such as oxygen has a larger tendency to become a neutral, rather than a cation. The study by Aiken et al. (2008) showed that the bias can be accounted for by dividing an average calibration factor (0.75) which was obtained from laboratory standards. However, a recent study found that the O/C values from the method of Aiken et al. (2008) are systematically biased low, particularly with larger biases for alcohols and simple diacids. Therefore, a new method on the basis of O/C from Aiken et al. (2008), fraction of CO_2^+ and CHO^+ was proposed for the calculation of O/C of organic aerosol (Canagaratna et al., 2015). To differentiate these two methods, the method of Aiken et al. (2008) was defined as “Aiken-Ambient” (A-A), and the one proposed by Canagaratna et al. (2015) was defined as “Improved-Ambient”. Following the reviewer’s suggestion, we defined A-A and I-A in the revised manuscript.

Page 23418: The discussion regarding aerosol acidity is almost certainly not correct. If the aerosol was acidic, it would be unable to support nitrate, which would partition completely to the gas phase as nitric acid. Reports of acidic aerosols in the atmosphere measured using AMS (e.g. in marine locations) always feature very little or no nitrate and show much worse correlations than is presented in figure 2. It is far more likely that in this instance, the aerosol is pH neutral and the sub-unity NH4 meas/pred value is because sulphate RIE used here is inaccurate. This parameter can and does vary from the default value of 1.2 and should have been calibrated along with the RIE of ammonium.

Thanks the reviewer’s comments. The default RIE (1.2) was used in this study for sulfate quantification. Unfortunately, we didn’t calibrate the AMS with pure $(NH_4)_2SO_4$ particles. As the reviewer mentioned, the RIE of sulfate might be a factor affecting the calculation of the predicted NH_4^+. In addition, a considerable fraction of

biomass burning was observed in this study which can emit chloride in the form of KCl. As a result, we may also overestimate the predicted NH_4^+ by counting all chloride as NH_4Cl, and hence overestimate aerosol particle acidity. The cations such as K^+ and Na^+, and the organic acids that the AMS cannot quantify will introduce further uncertainties in evaluating aerosol particle acidity. For these reasons, we deleted the discussions on aerosol particle acidity in the revised manuscript. We also deleted the section of aerosol particle acidity in Chen et al. (2015) which likely has the same issue.

Page 23420: Could the variation in the HOA/BC ratio also be caused by changes in the relative contributions from the local combustion sources such as biofuel, coal and traffic?

Thanks the reviewer's comment. Coal combustion was not a major source of organic aerosol during this study for two reasons: 1) the heating season in Beijing started from November 15 which was behind this study; 2) PMF analysis of high resolution mass spectra of organic aerosol did not resolve a factor associated with coal combustion emissions, while it can be resolved during the heating season (Sun et al., 2013). The reduction of BBOA (16%) during APEC was similar to that of HOA (19%), and the ratio of HOA/BBOA was 0.81 during APEC, which is also similar to that (0.84) before APEC. Therefore, we infer that the variations of HOA/BC ratios could not likely due to the changes of relative contributions of local combustion sources.

Haze event: Please use a different numbering convention than 'S1', 'S2', etc. for the stages because these are also used for the supplement figures and I found this confusing.

Thanks the reviewer's comment. The four stages were now defined as "E1, E2, E3, and E4" in the revised manuscript.

Figure 13: The vertically-resolved wind speed and direction data needs to be properly introduced. Is this the same data as was used in figure 14a of Chen et al.?

Yes, it is the same data as that in Chen et al. (2015). Following the reviewer's suggestion, we added a description of the wind profile measurements in the revised manuscript. "The wind profiles including WS and WD between 100 m to 5000 m were measured by a Doppler wind lidar (Windcube 200, Leosphere, Orsay, France) at the same location."

Figure 14: The caption needs to be specific about what event is being shown in this Figure

We revised the figure caption as:

Fig. 14. (a) Evolution of size distributions of sulfate, nitrate, and organics during the severe haze episode between October 22 and 25 (Fig. 12). (b) Average size distributions of sulfate, nitrate, and organics during the four stages of E1-E4.

Supplement: Are the ion tracers referred to in S1 and S2 derived from AMS data? If so, these are internal, not external tracers.

Good point. They were from the AMS measurements. We deleted “external” in the captions of Figs. S1 and S2.

Response to Referee #2

The manuscript reports detailed chemical characterization of PM_1, mostly NR-PM_1 during an important event (APEC) in Beijing. Strict atmospheric legislation emissions were imposed during APEC, which gave the authors the opportunity to investigate aerosol properties and sources before and during APEC, including severe haze episodes. The authors demonstrate experience on the techniques and provided very detailed information. Although not many new insights are presented, it seems to me that the results have implications on atmospheric chemistry and for this reason I recommend it to be accepted for publication in this journal after the considerations below are taken into account.

Thanks the reviewer's comments.

General comments:

Language was often poorly written, I recommend careful text revision, especially with the use of 'plural' form.

Thanks the reviewer's comments. We had a careful proofread in the revised manuscript.

In the introduction the authors claim that 'understanding of size distributions and elemental compositions of OA in Beijing remains poor'. Nowhere in this planet there have been so many studies with HR-AMS including HR-PMF, size distributions and elemental composition of OA till the present moment (I counted 8 studies!). No doubt that they were all important. However, I do not believe such sentences can be used as motivation statements.

Thank the reviewer's comments. HR-AMS has been widely used in field campaigns for characterization the size distributions and elemental composition of organic aerosols. Here we refer to the HR-AMS studies in Beijing. To our knowledge, the number of reported HR-AMS ambient studies in Beijing is approximately 9 (Huang et al., 2010a;Huang et al., 2010b;Liu et al., 2011;Zhang et al., 2014;Elser et al., 2015;Sun et al., 2015;Zhang et al., 2015a;Zhang et al., 2015b;Zhang et al., 2015c). Although several of these studies discussed the size distributions and elemental composition, most of them focused on the average size distributions for the entire study period and/or presented the time series and diurnal cycles of elemental ratios. Few of them discussed the evolution of size distributions during the severe haze episode, and also the evolution of oxidation degree of OA as a function of relative humidity was rarely investigated. Therefore, our understanding of the size

distributions and elemental composition of OA is still limited. Following the reviewer's comments, we revised this sentence as: "our understanding of the evolution of size distributions and elemental composition of OA in Beijing is still limited."

The authors say that emissions control during the Olympic Games 2008 were implemented to a lesser degree. Please provide more detail on that.

The emission controls during the Olympic Games included temporary closures of factories and restrictions on traffic by alternating the odd and even plate numbers. The control measures were mainly implemented in Beijing, while similar but less extensive traffic and industry restrictions were imposed in Beijing surrounding areas within a radius of about 150 km (Cermak and Knutti, 2009). In the revised manuscript, we added a more detailed description of the emission control during the Olympic Games and cited the reference of Cermak and Knutti (2009) for further details.

Limits of detection for the HR-AMS were estimated and presented, however, it surprises me that some compounds presented much lower values than the ones presented by DeCarlo et al. (2006), especially ammonium. Do the authors have an explanation for that?

There are several reasons for such differences: 1) the detection limits we reported are 5-min averages while those reported in DeCarlo et al. (2006) are 1-min values; 2) the detection limit of HR-AMS is instrument dependent. For example, the HR-AMS in DeCarlo et al. (2006) was the early version, while the performance of HR-AMS has been significantly improved during the last 10 years; 3) the ambient environment, e.g., relative humidity, might also be a factor affecting the detection limits, particularly ammonium, because the fragments of ammonium (mainly *m/z* 16, and 17) have interferences from water fragments (O^+ and OH^+). We removed the statement "which are close to the values reported in previous HR–AMS studies (DeCarlo et al., 2006) ." in the revised manuscript for clarification.

I suggest the authors include the input organics matrix dimensions, so the readers will know the number of variables and samples used in the PMF analysis. Also, explain if PMF was run for all the period (before APEC, during APEC) together or separately.

Good point. We clarified this information in the revised manuscript as:

"The PMF2.exe algorithm (v4.2) in robust mode (Paatero and Tapper, 1994) was applied to the HRMS matrix (4158×306) of OA for the entire study period to resolve distinct OA factors representing specific sources and processes."

In section 3.1 the authors say that nitrate contribution was larger than in previous studies. Is that an indication that legislation imposed during APEC was more effective for this compound? Why?

The higher nitrate contribution than those in previous studies indicate that nitrate played a more important role in PM pollution during the study period. One of the major reasons is the continuous reduction of SO_2 in recent years while the NO_x level remained at a high level and even increased. Another part of the reason is because of the season (autumn) for this campaign, when the temperature is not high enough to evaporate NH_4NO_3 substantially while the photochemical production is still strong (Zhang et al., 2012b). Based on our analysis, the emission controls over a regional scale during APEC showed similar impacts on nitrate and sulfate, and it is difficult to tell that the legislation imposed during APEC was more effective for nitrate reduction.

Concerning the acidity, do the authors have additional information concerning cations, such as K^+, Na^+, Rb^+? For example, Takegawa et al. (2009) measured those ions with tan AMS in Beijing. In an environment where mass loadings are so elevated, one could expect them to be relevant for the neutralization.

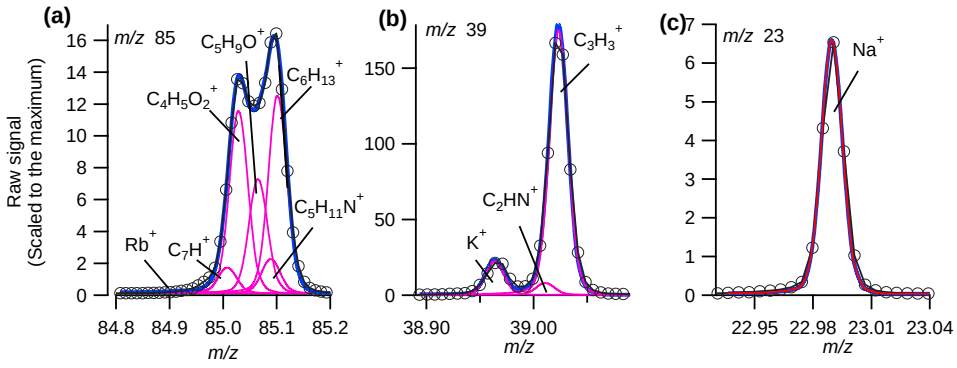

Figure R1. The raw spectra of (a) *m/z* 85 (b) *m/z* 39 and (c) *m/z* 23

The high resolution mass spectra showed clear signals of K^+ and Na^+ (Figure R1). However, quantification of K^+ and Na^+ is challenging due to the surface ionization

issue and also the unknown RIE of K^+ (RIE_K). The RIE_K can vary a lot depending on the tuning of the spectrometer and the temperature of the vaporizer. For example, Slowik et al. (2010) reported a RIE_K = 10 based on the calibration of pure KNO_3 particles using a ToF-AMS, which is much higher than the RIE_K = 2.9 obtained from the comparisons of K/S from fireworks and AMS measurements (Drewnick et al., 2006). In addition, the stability of surface ionization (SI) and electron impact (EI) also affects RIE_K. For these reasons, we didn't quantify K^+ and Na^+ with the HR-AMS measurements.

The K^+ and Na^+ will affect our evaluation of aerosol particle acidity in this study. For example, a considerable fraction of biomass burning was observed in this study which emits chloride mainly in the form of KCl. We may overestimate the particle acidity by counting all chloride as NH_4Cl. As the reviewer #1 mentioned, the RIE of sulfate and the organic acids may introduce further uncertainties in calculation of aerosol particle acidity. Therefore, we deleted the discussions on aerosol particle acidity in the revised manuscript.

Diurnal cycles of SIA components were very similar, increase in the afternoon. To me that suggests mixing layer development. Regional pollutants stay imprisoned above the mixing layer during the night and during the day when the mixing layer evolves they are released down to the surface level.

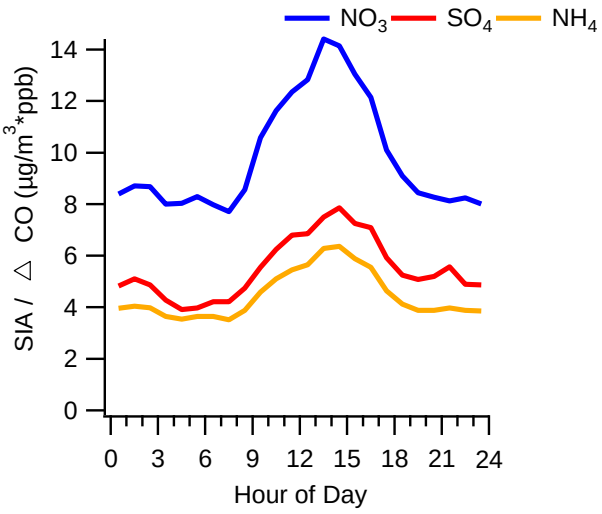

Figure R2. Diurnal cycles of SIA/△CO (△CO is the CO minus background CO).

As stated, planetary boundary layer (PBL) played an important role in changing the diurnal cycles of SIA components. Because of the stronger convective turbulence and higher temperature, the boundary layer height during daytime is generally much higher than that at night. The rising boundary layer would dilute the concentrations of pollutants leading to lower concentrations during daytime. Figure R2 shows the diurnal cycles of SIA/△CO which can remove the dilution effect of PBL to a certain degree. It is clear that secondary inorganic species showed pronounced daytime peaks indicative of daytime photochemical production. Therefore, the increased concentration of SNA in the afternoon was primarily caused by photochemical processing. It is possible that the pollutants in the residual layer at night can be mixed downwards to the ground site during daytime. However, we cannot draw such a conclusion based on the current data analysis in this study.

Concerning the COAs factors, the authors associate COA2 to charbroiling because that was the banned cooking technique during APEC. Could the authors provide further evidence of charbroiling cooking factor? For example, this factor presented CHN^+ *and* $CHNO^+$ *fragments, especially for larger m/zs (>m/z80). Any insights on what could those fragments represent? How could they be related to charbroiling and not to typical cooking?*

Thank the reviewer's comments. Charbroiling was banned in certain areas, e.g., Huairou district in Beijing during APEC. However the charbroiling activities were still significant in the streets near our sampling site. We currently don't have a good explanation for the high nitrogen-containing ions in cooking aerosols, which should be explored in the future by sampling directly the source aerosol of charbroiling.

Previous GC/MS analysis showed that unsaturated fatty acids were abundant organic aerosol species from Chinese cooking emissions (He et al., 2004;Zhao et al., 2006). The mass spectra of typical cooking organic aerosol are characterized by strong signal at *m/z* 41 and 55 (He et al., 2010), which is similar to the spectral profile of COA1. Whereas the spectrum of meat charbroiling showed high ion signals at *m/z* 43 and 55 (Mohr et al., 2009), which was similar to that of COA2 in our study. Based on these comparisons, we infer that COA1 was related to the typical cooking aerosol and COA2 was mainly associated with charbroiling.

It surprises me that all POA factors (but COA1) contain significant fractions of m/zs 60 and 73. Did the authors try ME2 to better separate the factors? They look rather mixed.

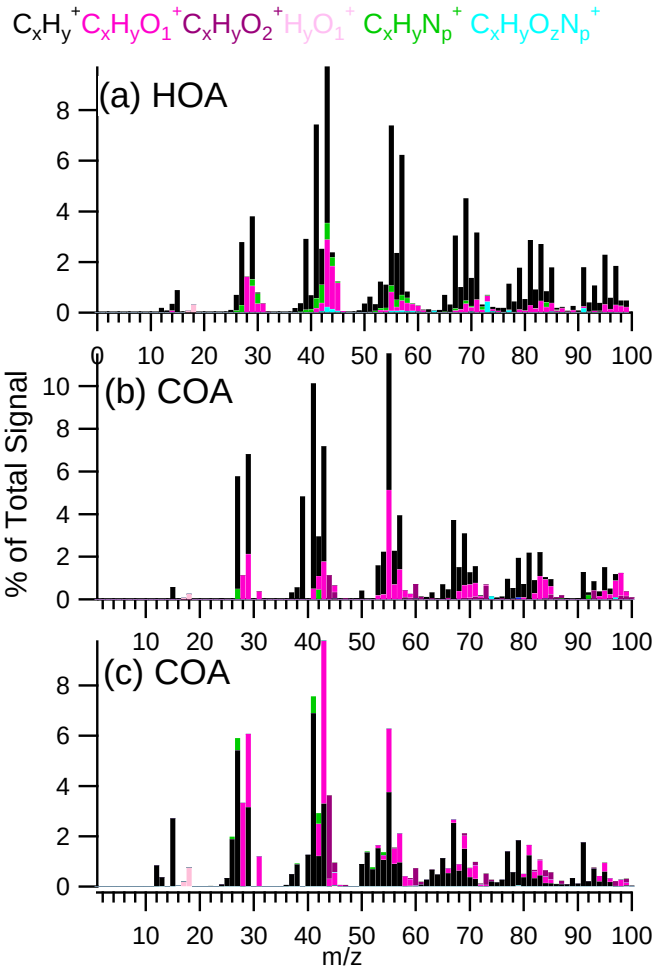

Figure R3. High-resolution mass spectra of OA resolved from previous studies, including (a) HOA (Aiken et al., 2009), (b) COA (Crippa et al., 2013) and (c) COA (Mohr et al., 2012).

Thank the reviewer's comments. We didn't try the advanced ME-2 analysis yet. The high *m/z* 60 in COA is consistent with that resolved in previous studies, e.g., Paris, 2009 (Crippa et al., 2013), Barcelona 2009 (Mohr et al., 2012), and also thsoe in source profiles of Chinese cooking emissions (He et al., 2010).

The high *m/z* 60 in HOA is not typical. However, the spectral patterns and the comparisons of time series with external tracers (CO and BC) indicate that the HOA factor was well separated. One explanation is that HOA was mixed with a small amount of coal combustion organic aerosol (CCOA) that cannot be resolved by PMF. The mass spectrum of CCOA is similar to that of HOA, yet shows visible *m/z* 60 peak

(Elser et al., 2015). However, due to their similar spectra and the small contribution of CCOA before the heating season, PMF analysis cannot resolve the CCOA factor.

Why was the terminology SV-OOA and LV-OOA utilized instead of OOAI and OOAII (Huang et al., 2010)? Both OOAs are very oxidized (m/z 44>43) and both present similar agreement with nitrate and/or SIA. It is not clear to me that the factor labeled as SV-OOA is more volatile. Concerning diurnal cycle of SV-OOA, how can the mountain valley breeze influence only this factor and not the others? Please explain.

The terms of "OOAI" and "OOAII" are widely used in early AMS, mostly Quadrupole-AMS studies which refer to highly oxidized and freshly oxidized oxygenated organic aerosol, respectively. Recent HR-AMS studies together with the volatility measurements (Huffman et al., 2009b;Huffman et al., 2009a;Jimenez et al., 2009) suggest that OOAI is characterized by high oxygen-to-carbon (O/C) ratio with low volatility while OOAII with lower O/C is found to be more volatile than OOAI. In addition, many studies found that OOAI often correlated with sulfate and OOAII often correlated with semi-volatile nitrate. Since then, the two types of OOA, i.e., OOAI and OOAII are commonly defined as low-volatility oxygenated organic aerosol (LV-OOA) and semi-volatile OOA (SV-OOA), respectively. In this study, the O/C of LV-OOA (=0.99) is much higher than that of SV-OOA (=0.47). To be consistent with previous studies, we named the two types of OOA as LV-OOA and SV-OOA, respectively. Although the two OOA both showed high *m/z* 44/43, we noticed a considerable fraction of $C_xH_y^+$ ions in SV-OOA, further indicating that it is less oxidized than LV-OOA.

The mountain-valley breeze influenced all OA factors as indicated by the diurnal cycles in Figure 6. All OA factors started to decrease from midnight when the mountain-valley breeze occurred.

SIA and OOA showed similar large accumulation modes peaking at 650nm. Usually, the lens transmission efficiency drops abruptly at D_{va}>600 nm. Please explain how could that be? Was the transmission efficiency measured for this instrument?

Thank the reviewer's comments. We didn't measure the lens transmission efficiency for our HR-AMS. One of the explanations is that there was a considerable amount of SIA and OOA in the larger particles, e.g., D_{va}>600 nm before APEC. In fact, a recent HR-AMS study using a $PM_{2.5}$ lens in Beijing (Elser et al., 2015) showed that the size distribution of sulfate during the pollution episode peaked at ~1000 nm while nitrate

showed the highest concentration between 600 – 1000 nm. Our study showed maximum sizes at ~650 nm for SIA which might indicate that the increased concentrations between 600 – 650 nm overcame the decreases caused by lens transmission efficiency. To be accurate, we revised "peaking at ~650 nm" as "peaking at ~650 nm or even larger".

In the Krevelen diagram, slopes before and during APEC are very similar (-0.52 and -0.58) to infer that different aging processes took place.

We agree with the reviewer that the slopes before and during APEC were similar. Therefore, we used "slightly" to describe the differences.

Minor Comments

P23414, L13: Write W-mode.

Changed

P23416, L17: NOx or NOy? In section 2.1.1 NOy was mentioned. Please choose one.

It is NO_x. NO and NO_y were measured by the gas analyzer (model 42i) from Thermo Scientific. The NO_2 was measured by a cavity attenuated phase shift NO_2 monitor (Aerodyne Research Inc.), which was described in section 2.1.1. The NO_x was then calculated as $NO_x=NO+NO_2$.

P23416, L19-22: Sentences need clarification. Were the two SV-OOAs combined? Please, write clarify.

We reworded this sentence as:

"The five-factor solution yielded a mixed SOA factor and the seven-factor solution split the SV-OOA into two components, which cannot be reasonably explained due to limited external tracers."

P23417, L11: 3rd, not '3'.

We changed it to "November 3".

P23417, L18: Write 'composed of' down.

Added.

P23417, L20: Did you mean organic mass fraction?

Yes, we revised it as “The contribution of organics showed a large increase, accounting for more than half of PM_1, whereas that of SIA was decreased from 51.2% to 35.4%.”

P23417, L27: Please report the NO_3/SO_4 value for Zhang, et al. (2014), so the reader can compare it.

Added.

P23419, L7: Spell out BA and DA.

Spelled out.

P23419, L23: Please cite few chloride combustion sources.

Added.

“Chloride, mainly from combustion sources, e.g., biomass burning and coal combustion (Levin et al., 2010;Zhang et al., 2012a), showed similar diurnal cycles before and during APEC”.

P23421, L4: The authors probably meant ‘increase’, not ‘decrease’. Please correct.

Corrected.

P23421, L17-18: Already described in section 2.1.1, no need to mention it again here.

Removed.

P23421, L21: The word correlates is not appropriate, replace it by ‘in agreement’.

Revised as “This result is consistent with the fact that vehicles use was limited only between 3:00 and 24:00 during APEC.”

P23427, L-14-15: This sentence is not clear.

It was reworded as “coinciding with a time without traffic control, and likely having more traffic emissions during APEC.”

P23432, L26: Please include the meteorological effects after emission control.

Added

Fig. 5 (f) right panel, there’s a typo, ‘SNA’.

We changed “SNA” to “SIA”.

Fig. 4 was cited after Fig 5 in the manuscript.

Changed

References

Aiken, A. C., DeCarlo, P. F., Kroll, J. H., Worsnop, D. R., Huffman, J. A., Docherty, K. S., Ulbrich, I. M., Mohr, C., Kimmel, J. R., Sueper, D., Sun, Y., Zhang, Q., Trimborn, A., Northway, M., Ziemann, P. J., Canagaratna, M. R., Onasch, T. B., Alfarra, M. R., Prevot, A. S. H., Dommen, J., Duplissy, J., Metzger, A., Baltensperger, U., and Jimenez, J. L.: O/C and OM/OC ratios of primary, secondary, and ambient organic aerosols with High-Resolution Time-of-Flight Aerosol Mass Spectrometry, Environ. Sci. Technol., 42, 4478-4485, 2008.

Aiken, A. C., Salcedo, D., Cubison, M. J., Huffman, J. A., DeCarlo, P. F., Ulbrich, I. M., Docherty, K. S., Sueper, D., Kimmel, J. R., Worsnop, D. R., Trimborn, A., Northway, M., Stone, E. A., Schauer, J. J., Volkamer, R. M., Fortner, E., de Foy, B., Wang, J., Laskin, A., Shutthanandan, V., Zheng, J., Zhang, R., Gaffney, J., Marley, N. A., Paredes-Miranda, G., Arnott, W. P., Molina, L. T., Sosa, G., and Jimenez, J. L.: Mexico City aerosol analysis during MILAGRO using high resolution aerosol mass spectrometry at the urban supersite (T0) - Part 1: Fine particle composition and organic source apportionment, Atmos. Chem. Phys., 9, 6633-6653, 2009.

Canagaratna, M. R., Jimenez, J. L., Kroll, J. H., Chen, Q., Kessler, S. H., Massoli, P., Hildebrandt Ruiz, L., Fortner, E., Williams, L. R., Wilson, K. R., Surratt, J. D., Donahue, N. M., Jayne, J. T., and Worsnop, D. R.: Elemental ratio measurements of organic compounds using aerosol mass spectrometry: characterization, improved calibration, and implications, Atmos. Chem. Phys., 15, 253-272, 10.5194/acp-15-253-2015, 2015.

Cermak, J., and Knutti, R.: Beijing Olympics as an aerosol field experiment, Geophys. Res. Lett., 36, 10.1029/2009gl038572, 2009.

Chen, C., Sun, Y. L., Xu, W. Q., Du, W., Zhou, L. B., Han, T. T., Wang, Q. Q., Fu, P. Q., Wang, Z. F., Gao, Z. Q., Zhang, Q., and Worsnop, D. R.: Characteristics and sources of submicron aerosols above the urban canopy (260 m) in Beijing, China during 2014 APEC summit, Atmospheric Chemistry and Physics Discussions, 15, 22889-22934, 10.5194/acpd-15-22889-2015, 2015.

Crippa, M., El Haddad, I., Slowik, J. G., DeCarlo, P. F., Mohr, C., Heringa, M. F., Chirico, R., Marchand, N., Sciare, J., Baltensperger, U., and Prévôt, A. S. H.: Identification of marine and continental aerosol sources in Paris using high

resolution aerosol mass spectrometry, Journal of Geophysical Research: Atmospheres, 118, 1950-1963, 10.1002/jgrd.50151, 2013.

DeCarlo, P. F., Kimmel, J. R., Trimborn, A., Northway, M. J., Jayne, J. T., Aiken, A. C., Gonin, M., Fuhrer, K., Horvath, T., Docherty, K. S., Worsnop, D. R., and Jimenez, J. L.: Field-Deployable, High-Resolution, Time-of-Flight Aerosol Mass Spectrometer, Anal. Chem., 78, 8281-8289, 2006.

Drewnick, F., Hings, S. S., Curtius, J., Eerdekens, G., and Williams, J.: Measurement of fine particulate and gas-phase species during the New Year's fireworks 2005 in Mainz, Germany, Atmos. Environ., 40, 4316-4327, 10.1016/j.atmosenv.2006.03.040, 2006.

Elser, M., Huang, R. J., Wolf, R., Slowik, J. G., Wang, Q. Y., Canonaco, F., Li, G. H., Bozzetti, C., Daellenbach, K. R., Huang, Y., Zhang, R. J., Li, Z. Q., Cao, J. J., Baltensperger, U., El-Haddad, I., and Prévôt, A. S. H.: New insights into PM_{2.5} chemical composition and sources in two major cities in China during extreme haze events using aerosol mass spectrometry, Atmospheric Chemistry and Physics Discussions, 15, 30127-30174, 10.5194/acpd-15-30127-2015, 2015.

He, L.-Y., Hu, M., Huang, X.-F., Yu, B.-D., Zhang, Y.-H., and Liu, D.-Q.: Measurement of emissions of fine particulate organic matter from Chinese cooking, Atmos. Environ., 38, 6557-6564, 10.1016/j.atmosenv.2004.08.034, 2004.

He, L. Y., Lin, Y., Huang, X. F., Guo, S., Xue, L., Su, Q., Hu, M., Luan, S. J., and Zhang, Y. H.: Characterization of high-resolution aerosol mass spectra of primary organic aerosol emissions from Chinese cooking and biomass burning, Atmos. Chem. Phys., 10, 11535-11543, 10.5194/acp-10-11535-2010, 2010.

Huang, X., Xue, L., He, L., Hu, M., Zhang, Y., and Zhu, T.: On-line measurement of organic aerosol elemental composition based on high resolution aerosol mass spectrometry, Chin. Sci. Bull., 55, 3391-3396, 10.1360/972010-1322, 2010a.

Huang, X. F., He, L. Y., Hu, M., Canagaratna, M. R., Sun, Y., Zhang, Q., Zhu, T., Xue, L., Zeng, L. W., Liu, X. G., Zhang, Y. H., Jayne, J. T., Ng, N. L., and Worsnop, D. R.: Highly time-resolved chemical characterization of atmospheric submicron particles during 2008 Beijing Olympic Games using an Aerodyne High-Resolution Aerosol Mass Spectrometer, Atmos. Chem. Phys., 10, 8933-8945, 10.5194/acp-10-8933-2010, 2010b.

Huffman, J. A., Docherty, K. S., Aiken, A. C., Cubison, M. J., Ulbrich, I. M., DeCarlo, P. F., Sueper, D., Jayne, J. T., Worsnop, D. R., Ziemann, P. J., and Jimenez, J. L.: Chemically-resolved aerosol volatility measurements from two megacity field studies, Atmos. Chem. Phys., 9, 7161-7182, 2009a.

Huffman, J. A., Docherty, K. S., Mohr, C., Cubison, M. J., Ulbrich, I. M., Ziemann, P. J., Onasch, T. B., and Jimenez, J. L.: Chemically-Resolved Volatility Measurements of Organic Aerosol from Different Sources, Environ. Sci. Technol., 43, 5351–5357, doi:10.1021/es803539d, 2009b.

Jimenez, J. L., Canagaratna, M. R., Donahue, N. M., Prevot, A. S. H., Zhang, Q., Kroll, J. H., DeCarlo, P. F., Allan, J. D., Coe, H., Ng, N. L., Aiken, A. C., Docherty, K. S., Ulbrich, I. M., Grieshop, A. P., Robinson, A. L., Duplissy, J., Smith, J. D., Wilson, K. R., Lanz, V. A., Hueglin, C., Sun, Y. L., Tian, J., Laaksonen, A., Raatikainen, T., Rautiainen, J., Vaattovaara, P., Ehn, M., Kulmala, M., Tomlinson, J. M., Collins, D. R., Cubison, M. J., E, Dunlea, J., Huffman, J. A., Onasch, T. B., Alfarra, M. R., Williams, P. I., Bower, K., Kondo, Y., Schneider, J., Drewnick, F., Borrmann, S., Weimer, S., Demerjian, K., Salcedo, D., Cottrell, L., Griffin, R., Takami, A., Miyoshi, T., Hatakeyama, S., Shimono, A., Sun, J. Y., Zhang, Y. M., Dzepina, K., Kimmel, J. R., Sueper, D., Jayne, J. T., Herndon, S. C., Trimborn, A. M., Williams, L. R., Wood, E. C., Middlebrook, A. M., Kolb, C. E., Baltensperger, U., and Worsnop, D. R.: Evolution of organic aerosols in the atmosphere, Science, 326, 1525-1529, doi:10.1126/science.1180353, 2009.

Levin, E. J. T., McMeeking, G. R., Carrico, C. M., Mack, L. E., Kreidenweis, S. M., Wold, C. E., Moosmüller, H., Arnott, W. P., Hao, W. M., Collett, J. L., Jr., and Malm, W. C.: Biomass burning smoke aerosol properties measured during Fire Laboratory at Missoula Experiments (FLAME), J. Geophys. Res., 115, D18210, 10.1029/2009jd013601, 2010.

Liu, Q., Sun, Y., Hu, B., Liu, Z., Akio, S., and Wang, Y.: In situ measurement of PM1 organic aerosol in Beijing winter using a high-resolution aerosol mass spectrometer, Chin. Sci. Bull., 1-8, 10.1007/s11434-011-4886-0, 2011.

Mohr, C., Huffman, J. A., Cubison, M. J., Aiken, A. C., Docherty, K. S., Kimmel, J. R., Ulbrich, I. M., Hannigan, M., and Jimenez, J. L.: Characterization of primary organic aerosol emissions from meat cooking, trash burning, and motor vehicles with High-Resolution Aerosol Mass Spectrometry and comparison with ambient and chamber observations, Environ. Sci. Technol., 43, 2443-2449, doi:10.1021/es8011518, 2009.

Mohr, C., DeCarlo, P. F., Heringa, M. F., Chirico, R., Slowik, J. G., Richter, R., Reche, C., Alastuey, A., Querol, X., Seco, R., Peñuelas, J., Jiménez, J. L., Crippa, M., Zimmermann, R., Baltensperger, U., and Prévôt, A. S. H.: Identification and quantification of organic aerosol from cooking and other sources in Barcelona using aerosol mass spectrometer data, Atmos. Chem. Phys., 12, 1649-1665, 10.5194/acp-12-1649-2012, 2012.

Paatero, P., and Tapper, U.: Positive matrix factorization: A non-negative factor model with optimal utilization of error estimates of data values, Environmetrics, 5, 111-126, 1994.

Slowik, J. G., Stroud, C., Bottenheim, J. W., Brickell, P. C., Chang, R. Y. W., Liggio, J., Makar, P. A., Martin, R. V., Moran, M. D., Shantz, N. C., Sjostedt, S. J., van Donkelaar, A., Vlasenko, A., Wiebe, H. A., Xia, A. G., Zhang, J., Leaitch, W. R., and Abbatt, J. P. D.: Characterization of a large biogenic secondary organic aerosol event from eastern Canadian forests, Atmos. Chem. Phys., 10, 2825-2845, 2010.

Sun, Y., Du, W., Wang, Q., Zhang, Q., Chen, C., Chen, Y., Chen, Z., Fu, P., Wang, Z., Gao, Z., and Worsnop, D. R.: Real-Time Characterization of Aerosol Particle Composition above the Urban Canopy in Beijing: Insights into the Interactions between the Atmospheric Boundary Layer and Aerosol Chemistry, Environ. Sci. Technol., 49, 11340-11347, 10.1021/acs.est.5b02373, 2015.

Sun, Y. L., Wang, Z. F., Fu, P. Q., Yang, T., Jiang, Q., Dong, H. B., Li, J., and Jia, J. J.: Aerosol composition, sources and processes during wintertime in Beijing, China, Atmos. Chem. Phys., 13, 4577-4592, 10.5194/acp-13-4577-2013, 2013.

Zhang, H., Wang, S., Hao, J., Wan, L., Jiang, J., Zhang, M., Mestl, H. E. S., Alnes, L. W. H., Aunan, K., and Mellouki, A. W.: Chemical and size characterization of particles emitted from the burning of coal and wood in rural households in Guizhou, China, Atmos. Environ., 51, 94-99, 10.1016/j.atmosenv.2012.01.042, 2012a.

Zhang, J., Wang, Y., Huang, X., Liu, Z., Ji, D., and Sun, Y.: Characterization of organic aerosols in Beijing using an aerodyne high-resolution aerosol mass spectrometer, Advances in Atmospheric Sciences, 32, 877-888, 10.1007/s00376-014-4153-9, 2015a.

Zhang, J. K., Sun, Y., Liu, Z. R., Ji, D. S., Hu, B., Liu, Q., and Wang, Y. S.: Characterization of submicron aerosols during a month of serious pollution in Beijing, 2013, Atmos. Chem. Phys., 14, 2887-2903, 10.5194/acp-14-2887-2014, 2014.

Zhang, J. K., Ji, D. S., Liu, Z. R., Hu, B., Wang, L. L., Huang, X. J., and Wang, Y. S.: New characteristics of submicron aerosols and factor analysis of combined organic and inorganic aerosol mass spectra during winter in Beijing, Atmospheric Chemistry and Physics Discussions, 15, 18537-18576, 10.5194/acpd-15-18537-2015, 2015b.

Zhang, J. K., Wang, L. L., Wang, Y. H., and Wang, Y. S.: Submicron aerosols during the Beijing Asia–Pacific Economic Cooperation conference in 2014, Atmos. Environ., 10.1016/j.atmosenv.2015.06.049, 2015c.

Zhang, Y., Sun, J., Zhang, X., Shen, X., Wang, T., and Qin, M.: Seasonal characterization of components and size distributions for submicron aerosols in Beijing, Science China Earth Sciences, 56, 890-900, 10.1007/s11430-012-4515-z, 2012b.

Zhao, Y., Hu, M., Slanina, S., and Zhang, Y.: Chemical Compositions of Fine Particulate Organic Matter Emitted from Chinese Cooking, Environ. Sci. Technol., 41, 99-105, 10.1021/es0614518, 2006.

Aerosol composition, ~~oxidative~~ oxidation properties, and sources in Beijing: results from the 2014 Asia-Pacific Economic Cooperation summit study

W. Q. Xu[1], Y. L. Sun[1,2*], C. Chen[1, 3], W. Du[1], T. T. Han[1], Q. Q. Wang[1], P. Q. Fu[1], Z. F. Wang[1], X. J. Zhao[4], L. B. Zhou[1], D. S. Ji[1], P. C. Wang[5], D. R. Worsnop[6]

[1]*State Key Laboratory of Atmospheric Boundary Layer Physics and Atmospheric Chemistry, Institute of Atmospheric Physics, Chinese Academy of Sciences, Beijing, China*

[2]*Collaborative Innovation Center on Forecast and Evaluation of Meteorological Disasters, Nanjing University of Information Science & Technology, Nanjing, China*

[3]*College of Applied Meteorology, Nanjing University of Information Science and Technology, Nanjing, China*

[4]*Institute of Urban Meteorology, China Meteorological Administration, Beijing, China*

[5]*Key Laboratory of Middle Atmosphere and Global Environment Observation, Institute of Atmospheric Physics, Chinese Academy of Sciences, Beijing, China*

[6]*Aerodyne Research, Inc., Billerica, Massachusetts, USA*

*Correspondence to Y. L. Sun (sunyele@mail.iap.ac.cn)

Abstract

The mitigation of air pollution in megacities remains a great challenge because of the complex sources and formation mechanisms of aerosol particles. The 2014 Asia-Pacific Economic Cooperation (APEC) summit in Beijing serves as a unique experiment to study the impacts of emission controls on aerosol composition, size distributions, and ~~oxidative~~ oxidation properties. Herein, a high-resolution time-of-flight aerosol mass spectrometer was deployed in urban Beijing for real-time measurements of size-resolved non-refractory submicron aerosol (NR-PM_1) species from October 14 to November 12, 2014, along with a range of collocated measurements. The average (±σ) PM_1 was 41.6 (±38.9) μg/m^3 during APEC, which was decreased by 53% compared with that before APEC. The aerosol composition showed substantial changes owing to emission controls during APEC. Secondary inorganic aerosols (SIA = sulfate + nitrate + ammonium) showed significant reductions of 62%–69%, whereas organics presented much smaller decreases (35%). The results from the positive matrix factorization of organic aerosols (OA) indicated that highly oxidized secondary OA (SOA) showed decreases similar to those of SIA during APEC. However, primary OA (POA) from cooking, traffic, and biomass burning sources were comparable to those before APEC, indicating the presence of strong local source emissions. The oxidation properties showed corresponding changes in response to OA composition. The average oxygen-to-carbon level during APEC was 0.36 (±0.10), which is lower than the 0.43 (±0.13) measured before APEC, demonstrating a decrease in the OA oxidation degree. The changes in size distributions of primary and secondary species varied during APEC. SIA and SOA showed significant reductions in large accumulation modes with peak diameters shifting from ~650 to 400 nm during APEC, whereas those of POA remained relatively unchanged. The changes in aerosol composition, size distributions, and oxidation degrees during the aging processes were further illustrated in a case study of a severe haze episode. Our results elucidated a complex response of aerosol chemistry to emission controls, which has significant implications that emission controls over

regional scales can substantially reduce secondary particulates. However, stricter emission controls for local source emissions are needed for further mitigating air pollution in the megacity of Beijing.

1. Introduction

Atmospheric aerosols, especially fine particles of particulate matter (PM) with aerodynamic diameters less than 2.5μm, play significant roles in human health hazards (Pope et al., 2009) and visibility reduction (Chow et al., 2002). Atmospheric aerosols also exert highly uncertain effects on climate change (Forster et al., 2007). Recently, the frequency of severe haze pollution events, which is characterized by high concentrations of fine particles, has become a significant concern in China (Zhang et al., 2010). Consequently, extensive studies have been conducted to investigate the sources, formation mechanisms, and evolution processes of haze pollution during the last decade. The results showed that fine particles were mainly composed of organic matter (OM) and secondary inorganic aerosols (SIA) including sulfate, nitrate, and ammonium. The major sources of $PM_{2.5}$ were also identified and quantified by using receptor models, e.g., factor analysis, chemical mass balance, positive matrix factorization (PMF) (Zheng et al., 2005;Song et al., 2006;Wang et al., 2008;Zhang et al., 2013), and tracer-based methods (Dan et al., 2004;Cao et al., 2005;Guo et al., 2012). Overall, traffic exhaust, industrial emissions, coal combustion, biomass burning, and secondary aerosols were the major sources of $PM_{2.5}$. Cooking aerosols (COA) werewas also found to be a significant contributor of $PM_{2.5}$ in urban environments (Huang et al., 2010b;Sun et al., 2010;Sun et al., 2013). Recent studies further highlighted the important roles of SIA and secondary organic aerosols (SOA) in the formation of severe haze pollution (Sun et al., 2014;Huang et al., 2014;Zheng et al., 2015). The substantial emissions from primary sources and rapid secondary aerosol formation coupled with stagnant meteorological conditions lead to frequent haze pollution in China, particularly during winter (Sun et al., 2014). However, because most previous studies are based on filter measurements with a time resolution ranging from hours to days, our knowledge of the rapid formation of severe haze

remains ~~poorly understood~~ limited. Although recent real-time measurements of aerosol composition have improved our understanding of the evolutionary processes of haze pollution, most of them focus on chemical composition and source analysis, and ~~.~~ ~~t~~The ~~oxidative~~ oxidation properties of aerosol particles remain ~~largely unknown.~~ less understood.

The aerodyne aerosol mass spectrometer (AMS) is unique for real-time characterization of size-resolved non-refractory submicron aerosol (NR-PM_1) composition (Jayne et al., 2000). The first deployments of Quadrupole AMS (QAMS) at urban (Sun et al., 2010) and rural sites (Yufa) (Takegawa et al., 2009) in Beijing in 2006 showed significant differences in aerosol chemical compositions between ~~such~~ the two sites. Organics dominated NR-PM_1 at both sites (33%–35%), whereas nitrate~~s~~ presented a much higher contribution at the urban site (22%) than at the rural site (11%). Three types of organic aerosols (OA) were identified : a hydrocarbon-like aerosol (HOA) from the primary emissions and two oxygenated OA (OOA) from the secondary formation (Sun et al., 2010). The results highlighted the importance of SOA in summer, which on an average contributed 61% of the total OA. The high-resolution time-of-flight AMS (HR–AMS), which provides more detailed chemical information and ~~oxidative~~ oxidation properties of OA, was first deployed in Beijing during the 2008 Olympic Game~~s~~ (Huang et al., 2010b). COA was first resolved by using AMS in Beijing and was observed to contribute a large fraction (25%) of the total OA. The elemental composition of OA factors was also determined. The oxygen-to-carbon (O/C) ratios of SOA (0.47–0.48) were significantly higher than those of primary OA (0.11–0.17), indicating significant~~ly~~ differences in the oxidation degrees of primary and secondary aerosols. Since 2008, the HR–AMS has been deployed in various environments, mainly in Beijing (Zhang et al., 2014a;Zhang et al., 2015), the Yangtze River Delta (YRD) (Huang et al., 2013), the Pearl River Delta (PRD) (He et al., 2011;Huang et al., 2011), and Lanzhou in northwest China (Xu et al., 2014). The average mass concentrations of submicron aerosols (PM_1) in China ranged from 15μg/m^3 to 67 μg/m^3 with organics constituting the major fraction (28%–52%)~~.~~

~~of PM_1~~. The OA ~~sources~~ factors ~~investigated~~ identified by ~~using~~ PMF analysis ~~,~~ include HOA, COA, biomass-burning (BBOA), coal combustion (CCOA) semi-volatile OOA (SV–OOA), and low-volatility OOA (LV–OOA). The OA factors varied substantially with seasons and sampling site environments.

Despite these results, few HR–AMS measurements have been reported in Beijing. Although the recent deployments of an aerosol chemical speciation monitor (ACSM) have illustrated the chemical evolution of aerosol species and OA factors in various seasons (Sun et al., 2012;Sun et al., 2013), our understanding of the evolution of size distributions and elemental compositions of OA in Beijing ~~remains poor mainly because of the limitations of ACSM~~ is still limited. Zhang et al. (2014a) reported a detailed characterizations of submicron aerosol composition, OA composition, and elemental composition of OA in January 2013. The results highlighted the vast differences in aerosol chemistry between clean and polluted days. Zhang et al. (2015) further analyzed two HR–AMS datasets collected in August and October in Beijing. The results showed higher oxidation degree of OA in summer than that in fall, in addition to differences in OA compositions during the two seasons.

Compared with previous HR–AMS measurements in Beijing, this study was conducted at a unique time during the Asia–Pacific Economic Cooperation (APEC) summit. To ensure good air quality during APEC, strict emission controls were implemented in Beijing and in the surrounding regions, which included restrictions on the number of vehicles in operation, factory operations, construction activities, and open barbeques. This study provides a unique opportunity to study the impacts of source emissions on aerosol chemistry in a megacity such as Beijing. Similar emission controls including temporary closures of factories and restrictions on traffic were implemented to a lesser degree during the 2008 Olympic Games (Cermak and Knutti, 2009). Numerous studies have investigated the impacts of emission controls on reductions in PM levels and secondary aerosol precursors during the Olympic Games. Emission controls were shown to significantly reduce primary aerosols and traffic- related gaseous and volatile organic compounds (Wang et al., 2010;Wang et al.,

2011;Shao et al., 2011;Guo et al., 2013), although the impacts on secondary species were significantly lower (Wang et al., 2010;Guo et al., 2013). In ~~studies designed to distinguish the relative contributions of emission controls from the effects of meteorological phenomena~~ addition, meteorological conditions were shown to play a more important role than emission controls in reducing PM levels during the Olympic Games (Wang et al., 2009;Cermak and Knutti, 2009). Therefore, significant uncertainties remain despite investigations of the response of aerosol chemistry to emission controls, and the link between emission controls and sources and the chemical composition of aerosol particles is far from being clearly understood.

In this study, we conduct real-time measurements of size-resolved NR–PM_1 composition by using an HR–AMS along with a suite of collocated instruments from October 14 to November 12, 2014. The submicron aerosol composition, diurnal variations, size distributions, elemental composition, and sources of OA are investigated in detail. In particular, the impacts of emission controls and meteorological variables on aerosol composition, size distributions, and ~~oxidative~~ oxidation properties are elucidated by comparing the aerosol chemistry before and during APEC. In addition, a comprehensive analysis is performed to illustrate the chemical evolution of aerosol properties during a severe haze pollution event.

2~~.~~ Experimental methods

2.1 Sampling and instrumentation

2.1.1 Sampling

This study took place from October 14 to November 12, 2014, at the Institute of Atmospheric Physics, Chinese Academy of Sciences, between the north 3rd and 4th ~~Ring~~ ring roads in Beijing. The HR–AMS was stored in a trailer near ground level with a sampling height of approximately 4m. Aerosol particles were sampled into the trailer at a flow rate of 10 L/min, of which ~0.1 L/min was isokinetically sampled into the HR–AMS. A $PM_{2.5}$ cyclone (model URG-2000-30EN) was mounted in front of the sampling line to remove coarse particles larger than 2.5 μm. In addition, aerosol particles were dried by a diffusion silica-gel dryer before sampling into the HR–AMS.

The collocated measurements in the trailer included particle extinction (630 nm) of $PM_{2.5}$ by a cavity attenuated phase shift extinction monitor (CAPS PM_{ext}, Aerodyne Research Inc.), gaseous NO_2 by a CAPS-NO_2 monitor, and black carbon (BC) by a two-wavelength ~~aethalometer~~ Aethalometer (model AE22, Magee Scientific Corp.). In addition, gaseous species (such as CO, O_3, NO, NO_y and SO_2) were simultaneously measured at a nearby two-story building by using a series of gas analyzers from Thermo Scientific. Meteorological parameters such as relative humidity (RH), temperature, wind speed (WS), and wind direction (WD) were obtained at 15 ~~elevations~~ heights ~~at~~ from the Beijing 325 m Meteorological Tower, which is approximately 30 m from the sampling site. The wind profiles including WS and WD between 100 m to 5000 m were measured by a Doppler wind lidar (Windcube 200, Leosphere, Orsay, France) at the same location. All of the data in this study are reported in Beijing Standard Time (BST), which is equivalent to Coordinated Universal Time (UTC) plus 8 h.

2.1.2 HR-AMS operations

The HR–AMS was operated by alternating the mass-sensitive V-mode and the high-mass-resolution ~~optical mode~~ W-mode every 5min. Under V-mode operation, the HR–AMS cycled through the mass spectrum (MS) and particle time-of-flight (PToF) modes every 10 s. No PToF data were collected in the W-mode due to the limited signal-to-noise (S/N) ratio. The particle-free ambient air was sampled and analyzed to determine the detection limits (DLs) of NR–PM_1 species and the fragment ion ratios of gases for subsequent high-resolution analysis. The 5 min DLs of organics, sulfate, nitrate, ammonium, and chloride of V and W-modes determined as three times the standard deviations (3σ) were 0.017, 0.010, 0.0016, 0.0014, and 0.004μg/m^3 and 0.030, 0.035, 0.026, 0.0049, and 0.032μg/m^3, respectively~~,~~. ~~which are close to the values reported in previous HR–AMS studies (DeCarlo et al., 2006).~~ Prior to this study, the ionization efficiency (IE) and particle sizes were calibrated ~~by~~ using pure ammonium nitrate particles and polystyrene latex spheres (PSL, density = 1.05 g/cm^3), respectively, following previous standard protocols (Jayne et al., 2000;Jimenez,

2003;Drewnick et al., 2005).

2.2 HR-AMS data analysis

The mass concentrations and size distributions of NR–PM_1 were analyzed by using standard AMS data analysis software (SQUIRREL v1.56 and PIKA v 1.15D) written in Igor Pro 6.12A (Wavemetrics, Lake Oswego, Ore., USA). A constant collection efficiency (CE) of 0.5 was applied for the quantification of NR–PM_1 species because ~~the~~ aerosol particles were dry and were slightly acidic as indicated by $NH_4^+{}_{measured}/NH_4^+{}_{predicted}$ (= 0.75) (Zhang et al., 2007). In addition, the overall mass fractions of ammonium nitrate were below the threshold value (40%) that significantly affects the CE (Matthew et al., 2008). Therefore, the three major factors, humidity, particle acidity, and ammonium nitrate fraction, did not significantly affect the universal CE = 0.5, which has been widely used in numerous AMS studies. However, a constant CE value may introduce an uncertainty of 20%–30% for the mass concentrations of NR–PM_1 species (Middlebrook et al., 2012). The default relative ionization efficiencies (RIEs) of 1.4 for organics, 1.2 for sulfate, 1.1 for nitrate, and 1.3 for chloride were used (Allan et al., 2003) in this study; that for ammonium, 5.0, was determined from pure NH_4NO_3 particles. The total PM_1 mass (= NR−PM_1 + BC) agreed well with $PM_{2.5}$ (R^2 = 0.86). The average ratio of $PM_1/PM_{2.5}$, 0.77, was also consistent with that reported in previous studies (Sun et al., 2014). This result further supports that CE = 0.5 is reasonable for this study.

The high-resolution mass spectra (HRMS) of the V- and W-modes were analyzed for ion-speciated fragments of $C_xH_y^+$, $C_xH_yO_z^+$, $C_xH_yN_p^+$, and $C_xH_yO_zN_p^+$ ~~by~~ using PIKA v1.15D. The elemental composition of OA, including ratios of oxygen-to-carbon (O/C), hydrogen-to-carbon (H/C), organic mass to organic carbon (OM/OC), and nitrogen-to-carbon (N/C), were determined by using the elemental analysis approach recommended by Aiken et al. (2007), referred to here as "Aiken-Ambient"(A-A). We also calculated the elemental ratios ~~by~~ using the improved calibration factors recommended by Canagaratna et al. (2015), referred to here as "Improved-Ambient"(I-A). The average A-A H/C and O/C ratios were 1.55

and 0.41, which are respectively 8% and 20% lower than the I-A H/C and O/C ratios of 1.69 and 0.51. For consistency with previous studies, the elemental composition determined ~~by using~~ from the A-A approach was reported in this study. ~~In addition, the oxidation state ($\overline{OS}$ = 2 × O/C−H/C) (Kroll et al., 2011) of OA was calculated to be =0.73 and =0.67 with the A-A and I-A methods, respectively.~~

The PMF2.exe algorithm (v4.2) in robust mode (Paatero and Tapper, 1994) was applied to the HRMS matrix (4158 × 306) of OA for the entire study period to resolve distinct OA factors representing specific sources and processes. Values of *m/z* larger than 120 were excluded due to the limited mass resolution in separating higher mass ions. Isotopic ions scaled on the basis of the signals of parent ions were also excluded. Such exclusion had a minor impact on the total mass (~2–3%). Other data-pretreatments were similar to those reported in previous studies; that is, the bad ions with S/N <0.2 were removed, and the "weak" ions with 0.2 < S/N < 3 were further down-weighted by increasing their errors by a factor of three.

The PMF solutions were investigated in detail by evaluating the mass spectral profiles and time series of OA factors (1 to 10) as a function of rotational parameter (fPeak). By comparing the mass spectral profiles of OA factors with previously reported standard mass spectra, and the time series with external tracers, such as CO, NO_x, BC, SIA, $C_3H_5O^+$, and $C_2H_3O^+$, a six-factor solution with fPeak=0 was selected in this work. ~~Although T~~the five-factor solution yielded a mixed SOA factor and ~~was a mixed factor for the five-factor solution,~~ the seven-factor solution split the SV-OOA into two components, which cannot be reasonably explained due to limited external tracers. A ~~Summary~~ summary of the key diagnostic plots of the PMF results ~~are~~ is shown in Figs. S1–S3.

3~~.~~ Results and discussion

3.1 Mass concentrations and chemical composition

Figure 1 shows the time series of submicron aerosol species during the entire study period. All aerosol species varied dramatically between haze episodes and clean periods. As indicated in the figure, three evident pollution episodes and two episodes

were observed before and during APEC, respectively. The formation and evolution of the haze episodes were closely related to stagnant meteorology characterized by low WS and high RH. The average (±σ) mass concentration of PM_1 was 41.6 (±38.9) $\mu g/m^3$ during APEC, which was 52.7% lower than the 88.0 $\mu g/m^3$ measured before APEC. Periods of high PM_1 concentration (>60 $\mu g/m^3$) accounted for 56.7% of the time before APEC and 22.6% during APEC. These results indicate significant reductions in PM during APEC, particularly for pollution events with high PM_1 loading.

The variations of inorganic aerosol and organics showed different behaviors before and during APEC. Figure 1c shows clear decreases in inorganic aerosol species on November 3, when emission controls were first implemented in Beijing. Relatively low ambient levels were maintained on November 6, when far stricter emission controls were imposed in Beijing and in the surrounding regions. As a comparison, the variations in organics were more dramatic, and the changes during APEC were not as significant as those for inorganic aerosol species. Although SIAs such as sulfate, nitrate, and ammonium were decreased by 62 – 69% during APEC, organics showed a much smaller decrease of 35% (Table 1). The chemical composition of PM_1 before APEC was mainly composed of organics, accounting for 38.0%, followed by nitrate at 26.4% and sulfate at13.7%. The average aerosol composition during APEC showed significant changes. The contribution of ~~O~~organics showed a large increase, accounting for more than half of PM_1, whereas ~~the contribution~~that of SIA was decreased from 51.2% to 35.4%. These results suggest different responses of SIA and OA to emission controls. However, the measurements at 260 m at the same location showed significant decreases of 40–80% for all aerosol species during APEC, whereas the bulk aerosol composition was relatively similar before and during APEC as a result of synergetic controls of aerosol precursors over a regional scale (Chen et al., 2015). These results indicated the different sources of aerosol particles between the ground site and 260 m. Compared with ~~that reported in~~ previous AMS studies in Beijing, we observed a significantly higher nitrate contribution before APEC in

summer 2008 (15.8%)(Huang et al., 2010b) and in winter 2011–2012 (16.0%) (Sun et al., 2013). The average mass ratio of NO_3/SO_4 was 1.78, which is also significantly higher than the values (0.78-1.04) previously reported in China (Zhang et al., 2012b;Zhang et al., 2014b). High nitrate contribution to PM_1 was also observed at 260 m, which accounted for 27% and 29%, respectively before and during APEC (Chen et al., 2015). Thus, our results elucidate the important role of nitrate in PM pollution during the study period.

~~Figure 2 shows a correlation between measured NH_4 ($NH_4^+{}_{measured}$) and predicted NH_4^+ ($NH_4^+{}_{predicted}$) required to fully neutralize sulfate, nitrate, and chloride (= 18 × (2 × SO_4/96 + NO_3/62 + Chl/35.5))(Zhang et al., 2007). A ratio of $NH_4^+{}_{measured}$ / $NH_4^+{}_{predicted}$ less than 1 indicates acidic aerosol particles. As shown in Fig. 2, the average ratio of $NH_4^+{}_{measured}$ / $NH_4^+{}_{predicted}$ was 0.75 before APEC, indicating that aerosol particles were overall acidic during this study. The aerosol particle acidity was similar to that observed in January 2013 with $NH_4^+{}_{measured}$ / $NH_4^+{}_{predicted}$ ratios varying between 0.66 and 0.74 (Zhang et al., 2014a). $NH_4^+{}_{measured}$ also correlated strongly with $NH_4^+{}_{predicted}$ (R^2 = 0.99) during APEC, yielding a regression ratio of 0.80. This result suggests a slight decrease in aerosol particle acidity during APEC, which is likely attributed to a reduction in precursors of NO_2 and SO_2, and hence a decrease in the formation of sulfate and nitrate during APEC. An additional factor is that the oxidation of precursors to SIA, e.g., aqueous phase processing of SO_2, was slower owing to lower RH during APEC. Nevertheless, it appears that the joint controls of SIA precursors over a regional scale did not significantly affect the aerosol particle acidity.~~

3.2 Diurnal cycles

The diurnal cycles of PM_1 species before and during APEC are illustrated in Fig.~~3~~2. SIA showed similar pronounced diurnal cycles before APEC, which were all characterized by gradual increases during daytime. Such diurnal cycles were primarily driven by photochemical processing, considering the rising planetary boundary layer height during daytime. Similar diurnal cycles of SIA were also observed during winter

312 in 2011–2012 (Sun et al., 2013). Note that the ratio of NO_3/SO_4 was not constant
313 throughout the day. In fact, a gradual decrease in NO_3/SO_4 from ~2.2 to 1.9 was
314 observed during daytime, indicating additional evaporative loss of nitrate particles
315 because of gas–particle partitioning. The diurnal cycles of SIA during APEC differed
316 significantly. The concentrations of SIA at night were nearly twice that during the day.
317 A detailed check of the meteorology and time series of aerosol species during APEC
318 revealed that the routine circulation of mountain–valley breeze played a dominant role
319 in driving the diurnal variations. As indicated in Fig. 1, a northwesterly
320 mountain–valley breeze occurred regularly at midnight on November 9–10 when the
321 mass concentrations of aerosol species began to decrease. The mountain–valley
322 breeze dissipated at approximately noon when the WD changed from the northwest to
323 the south, and the mass concentrations reached the minimum daily level.
324 Consequently, the change percentages of SIA (~~= ([BA] – [DA])/[BA]~~=([Before
325 APEC]-[During APEC])/([Before APEC])) showed pronounced diurnal cycles with
326 the greatest decrease during daytime. Because SIA was formed mainly over a regional
327 scale and was less influenced by local sources, we can roughly estimate the relative
328 contributions of emission controls and mountain–valley breeze effects. Assuming that
329 the decreases in SIA during APEC were caused mainly by emission controls and the
330 mountain–valley breeze, and that the decreases in SIA at night without the
331 mountain–valley breeze were caused solely by emission controls, we can estimate that
332 approximately 27% of reduction in sulfate and nitrate during the day was caused by
333 the cleaning effects of the mountain–valley breeze.
334 Organics showed a substantially different diurnal cycle from that of SIA,
335 characterized by a pronounced nighttime peak and a visible noon peak. The diurnal
336 cycles of OA factors indicated that such diurnal variations were mainly driven by
337 local primary sources such as cooking, traffic, and biomass burning emissions.
338 Although organics showed a decrease of approximately 60% during daytime, the
339 differences before and during APEC were much smaller at nighttime, indicating that
340 strong local sources emissions remained during APEC despite the strict emission

controls. Chloride, mainly from combustion sources, e.g., biomass burning and coal combustion (Levin et al., 2010;Zhang et al., 2012a), showed similar diurnal cycles before and during APEC with the greatest reduction occurring during daytime. Similarly, the small decrease in chloride at nighttime likely indicates the presence of a considerable amount of combustion emissions during APEC. The diurnal cycles of BC were similar before and during APEC, both characterized by significantly higher concentrations at nighttime that during the day. Such a diurnal cycle of BC is similar to that previously observed in Beijing (Han et al., 2009), indicating higher BC source emissions during night time. This result is consistent with the diurnal variations of diesel trucks and heavy-duty vehicles that are only allowed to operate inside the city between 22:00–6:00. Different from other aerosol species, the reduction in BC was relatively constant at 47.0–67.5% throughout the day, suggesting similar BC sources before and during APEC, but with different emission intensities. In addition, the mountain–valley breeze effect on BC was different from that on other species, likely due to the similar BC levels in northwest and south Beijing.

3.3 Composition and sources of OA

Six OA factors were identified by PMF analysis of HRMS of OA, including four primary OA factors (HOA, BBOA, COA1, and COA2), and two secondary OA factors (SV-OOA and LV-OOA). The mass spectra and time series of the six OA factors are shown in Fig. ~~5~~3.

The HOA spectrum was characterized by prominent hydrocarbon ion series of $C_nH_{2n+1}^+$ and $C_nH_{2n-1}^+$, which is consistent with that observed at various urban sites (Huang et al., 2010b;Sun et al., 2011b;Xu et al., 2014). The O/C ratio of HOA was 0.17, which is considerably higher than 0.03–0.04 measured from diesel and gasoline exhausts (Mohr et al., 2009) and slightly higher than 0.11–0.13 observed in the YRD (Huang et al., 2013), and the PRD in China (He et al., 2011), indicating that the HOA in this study was relatively oxidized. HOA correlated well with BC ($R^2 = 0.78$) during APEC, and the average HOA/BC ratio of 1.2 was consistent with that obtained in other megacities such as Mexico City (Aiken et al., 2009) and New York City (Sun et

al., 2011b). Although HOA also tightly correlated with BC before APEC (R^2 = 0.66), a significantly lower ratio of HOA/BC (0.57) was observed. These results suggest a substantial change of the sources of either HOA or BC during APEC. As shown in Fig. ~~3~~2, BC showed large reductions similar to those of SIA during APEC, suggesting that a large fraction of BC was likely from regional transport. This result is consistent with a recent study at an urban site in Lanzhou (Xu et al., 2014) in which 53% of BC was found to be associated with SIA and SOA ~~at an urban site in Lanzhou~~, and the rest 47% was from local primary emissions. Therefore, we infer that the HOA/BC ratio of 1.2 during APEC is likely representative of local source emissions, whereas lower HOA/BC ratios before APEC indicate additional BC sources such as regional transport. Therefore, the HOA/BC ratio can be used to indicate the relative importance between local emissions and regional transport. The ~~decrease~~ increase in the HOA/BC ratio during APEC illustrates a significant reduction of BC from regional transport owing to emission controls over a regional scale. Sun et al. (2014) also reported a large decrease in the HOA/BC ratio during severe haze episodes in which approximately 53% of BC was from regional transport.

The HOA/CO ratios were similar before and during APEC, at 1.64 and 1.40, respectively, but were significantly lower than the values reported in Mexico City (Aiken et al., 2009) and Fresno, California (Ge et al., 2012b) at 5.71 and 5.64, respectively. A likely explanation is that more complex sources of CO from traffic, cooking, and biomass burning were measured in this study. Indeed, HOA only correlated moderately with CO (R^2 = 0.39) before APEC. HOA showed similarly pronounced diurnal cycles before and during APEC with nighttime concentrations approximately four – six times that during the day (Fig. ~~6~~5). The diurnal cycle of HOA resembled that of BC, yet the reduction during APEC was significantly smaller, ranging from ~20% to 50% between 9:00 and 24:00. ~~All of the data in this study are reported in Beijing Standard Time (BST), which is described in Sect. 2.1.1.~~ Note that the HOA concentration between 0:00 and 3:00 during APEC was even slightly higher than that before APEC, indicating the presence of emissions from diesel trucks and

heavy-duty vehicles during this period. This result ~~correlates~~ is consistent with the fact that vehicles use was limited only between 3:00 and 24:00 during APEC.

The mass spectra of the two COA factors were both characterized by high ratios of *m/z* 55/57, at 2.4 and 2.1, respectively, which is consistent with the spectral characteristics of fresh cooking aerosols (Mohr et al., 2009;He et al., 2010) and that of COA ubiquitously observed in megacities (Huang et al., 2010b;Sun et al., 2011a;Ge et al., 2012a). As shown in Fig. ~~5~~3, the O/C of COA1 was 0.07, which is significantly lower than 0.19 of COA2, suggesting significant differences in ~~oxidative~~ oxidation properties. Moreover, COA1 correlated more strongly with the tracer ion $C_6H_{10}O^+$ of COA (Sun et al., 2011b) (R^2 = 0.96) than COA2 (R^2 = 0.81–0.83), which is indicative of their different sources. The diurnal cycles of COA1 and COA2 were both characterized by pronounced evening peaks with maximum concentrations occurring between 20:00 and 21:00, indicating the large amount of cooking activities at nighttime. Note that the diurnal cycle of COA1 showed clear morning and noon peaks associated with breakfast and lunch emissions, which were almost invisible for COA2. Interestingly, a significant decrease in COA1 concentration was not observed during APEC, suggesting similar local cooking sources near the sampling site before and during APEC. However, COA2 showed a considerable reduction from late afternoon to mid-night during APEC. This result suggests that the sources of COA2 were controlled by a certain degree during APEC. Considering that the major control of cooking emissions was the banning of open charcoal grills, we conclude that the COA2 was primarily from charbroiling emissions, whereas COA1 was more like a factor of regular cooking emissions.

The BBOA spectrum showed pronounced peaks at *m/z* 60, mainly $C_2H_4O_2^+$, and *m/z* 73, mainly $C_3H_5O_2^+$; these two maker ions indicate the presence of biomass burning (Alfarra et al., 2007;Aiken et al., 2009;Cubison et al., 2011). BBOA correlated strongly with $C_2H_4O_2^+$ before and during APEC (R^2 = 0.65 and 0.88, respectively). The weaker correlation before APEC is likely due to other source contributions to $C_2H_4O_2^+$ such as cooking aerosol (COA2). The O/C ratio of BBOA

was 0.50, which is significantly higher than that observed in Kaiping and Jiaxing in China at 0.26–0.27 (Huang et al., 2011;Huang et al., 2013), and in Mexico City at 0.30 (Aiken et al., 2009). The f_{44} of BBOA, at 11.3% was higher as well. Because biomass burning, e.g., agricultural burning in October, was rare inside the city of Beijing, the observed BBOA was expected to be mainly from regional transport. Previous studies have shown that BBOA can be rapidly oxidized in the atmosphere, leading to a decrease in f_{60} and a corresponding increase in f_{44} (Cubison et al., 2011). Therefore, we infer that BBOA in this study was an aged BBOA from regional transport. In fact, the O/C ratio of BBOA was close to that of the aged BBOA observed from the aircraft measurements during the Megacity Initiative: Local and Global Research Observations (MILAGRO) project in 2006 (DeCarlo et al., 2010). The diurnal cycles of BBOA ~~were~~ differed substantially before and during APEC. Although relatively flat before APEC, it presented a pronounced diurnal variation with nighttime concentration approximately three times that during daytime. Although the daytime BBOA concentration was reduced by ~40% during APEC, the nighttime concentration was even higher than that before APEC. These results suggest that significant biomass burning emissions remained in the surrounding regions of Beijing during APEC. The low daytime concentration was found to be mainly associated with the mountain–valley breeze that carried aerosols from the northwest with significantly lower biomass burning emissions to Beijing.

Compared with POA, the two OOA factors, SV-OOA and LV-OOA, showed significantly higher f_{44} and O/C ratios. The f_{44} and O/C of LV-OOA were 0.22 and 0.99, respectively, indicating that LV-OOA was a highly aged SOA. Indeed, the O/C of LV-OOA in this study was even higher than that previously observed at various urban sites in China, e.g., Shanghai, Lanzhou, Shenzhen, and Hong Kong at ~0.6–0.8 (He et al., 2011;Huang et al., 2012;Lee et al., 2013;Xu et al., 2014). LV-OOA highly correlated with SIA before and during APEC (R^2 = 0.98 and 0.94, respectively), indicating the secondary nature of LV-OOA. The diurnal cycle of LV-OOA before APEC showed a gradual increase during daytime, although the absolute increase at ~4

μg/m^3 was significantly smaller than the background concentration at ~ 8 μg/m^3. This result indicates that LV-OOA was mainly from regional transport, which is consistent with its high ~~oxidative~~ oxidation properties. Comparatively, LV-OOA showed a similar diurnal cycle as that of SIA during APEC characterized by a higher concentration at nighttime. As indicated in Fig. 4, LV-OOA showed the greatest reduction among OA factors, at 60–80%, which indicates that regional emission controls exerted the most impact on LV-OOA. SV-OOA showed moderately high f_{44} and O/C at 0.15 and 0.47 respectively, suggesting a lesser degree of photo-chemical processing. SV-OOA correlated with nitrate (R^2 = 0.50), indicating similar semi-volatile properties (Ulbrich et al., 2009). However, significant differences in variation between SV-OOA and nitrate were also observed occasionally. In particular, the time series of SV-OOA showed sporadic peaks corresponding to those of COA, BBOA, and HOA, yet they were not observed in the nitrate time series. These results might suggest that part of freshly emitted OA can be rapidly oxidized to form SV-OOA. The diurnal cycle of SV-OOA before APEC showed an evident daytime increase, indicating photochemical processing. However, such a diurnal cycle was not observed during APEC. These results indicated that photochemical processing was not the major factor driving the diurnal variation of SV-OOA during APEC. In fact, we determined that the mountain–valley breeze played a more important role.

Overall, SOA dominated the OA composition before APEC with SV-OOA and LV-OOA accounting for 24.4% and 30.0%, respectively. POA together accounted for 45.4% of the total OA with cooking aerosol being the largest component at 23%. It should be noted that the COA contribution varied significantly throughout the day. Although COA showed a contribution of generally less than 20% during daytime, its contribution reached as high as 40% at dinner time (Fig.4). BBOA also comprised a considerable fraction of OA, at 12.2% on average. The average mass concentrations of SV-OOA and LV-OOA showed large decreases by 56% and 74%, during APEC, respectively (Table 1), whereas those of primary OA showed significantly lower decreases ranging from 16% to 27%. As a result, the bulk OA composition showed a

substantial change during APEC. For example, the contribution of SOA decreased from 54% before APEC to 34% during APEC. Correspondingly, all primary OA factors showed elevated contributions to OA. As a comparison, POA at 260 m with much less influences from local sources showed a similar reduction to SOA (Chen et al., 2015). Our results have significant implications ~~such~~ that controlling secondary precursors over regional scales can reduce secondary particulates substantially and hence mitigate air pollution in megacities. As previously discussed, the reduction of local primary emissions was significantly less than that of secondary aerosol during APEC; therefore, stricter control of local source emissions is crucial for improving air quality in the future.

The RH and wind dependence of SV-OOA and LV-OOA before and during APEC are shown in Fig. ~~7~~6. Both SV-OOA and LV-OOA showed clear concentration gradients as a function of RH with higher concentrations associated with higher RH levels. The lowest concentrations of SV-OOA and LV-OOA were observed at low RH levels (<30%) with northerly winds. No significant differences in SOA, particularly LV-OOA, were noted between the south and the north when the WS (280 m) was less than 4 m/s and the RH was above 60%, indicating that SOA was relatively evenly distributed around the sampling site under stagnant meteorological conditions. The ratio of LV-OOA/SV-OOA was larger than 1 for most of the time at RH >60%, suggesting a more important role of highly oxidized SOA at high RH levels. In contrast, SV-OOA was more important than LV-OOA at low RH levels. SV-OOA and LV-OOA during APEC generally showed similar RH- and wind-dependent patterns (Figs. ~~7b~~6b, d). By comparing the SV-OOA and LV-OOA before and during APEC under similar RH and wind conditions, we can evaluate the impacts of emission controls on SOA. Both SV-OOA and LV-OOA showed significant reductions at RH > 40% suggesting that regional emission controls played a significant role in suppressing the formation of SOA. However, small changes and even increases of SV-OOA and LV-OOA in the low RH region from the north were observed, which is consistent with the fact that emission controls were implemented mainly in the

regions south of Beijing. Figure ~~7f~~ 6f shows a very different ratio of LV-OOA/SV-OOA during APEC. In particularly, SV-OOA was higher than LV-OOA for most of the time, indicating that SOA was less oxidized during APEC.

3.4 Size distributions

Figure ~~8~~ 7 presents the average mass-weighted size distributions of NR-PM_1 species before and during APEC. The size distributions of OOA were derived from that of *m/z* 44 by normalizing the integrated signals of *m/z* 44 between 30 nm and 1500 nm to the concentrations of OOA (Zhang et al., 2005). This method is rational because *m/z* 44 (mainly CO_2^+) strongly correlated with OOA (R^2=0.98). The size distributions of POA were then obtained from the differences between total OA and OOA. It should be noted that the OOA concentration might be slightly overestimated in small size ranges because ~17% of *m/z* 44 was constituted by POA. SIA and OOA showed similar single large accumulation modes peaking at ~650 nm or even larger before APEC. In comparison, POA showed a much broader size distribution with the peak diameter occurring at ~300 nm. The size-resolved composition showed a dominant contribution of POA in small size ranges, accounting for almost 80% below 100 nm, whereas the contributions of SIA and OOA increased significantly from ~20% to more than 90% as the particle diameter increased from 100 nm to 1000 nm. These results indicate the dominant contributions of secondary aerosol to accumulation mode particles, whereas primary emissions played more significant roles in ultrafine mode particles. The differences in size distributions between POA and secondary aerosol also highlight their different sources and aging processes.

The size distributions of SIA and OOA showed substantial changes during APEC. Although the mass concentrations in the accumulation mode were reduced by approximately 50%, the peak diameters also shifted to smaller sizes (~400 nm). These results demonstrate that emission controls of secondary aerosol precursors exerted a dominant impact on accumulation mode particles. As indicated in Fig. 1, the duration time of pollution episodes before APEC was overall longer than that during APEC, indicating that secondary aerosol was less aged during APEC. This might also

explained the smaller size of secondary aerosol species during APEC. In addition, we noted that the average RH during APEC was 37%, which is lower than 53% recorded before APEC. The relatively drier conditions during APEC also played a role in suppressing particle growth. Indeed, clear particle growth was observed during three episodes before APEC, although it was insignificant during APEC. Comparatively, the size distribution of POA remained relatively unchanged, indicating the presence of strong local source emissions during APEC. This result is consistent with the significantly smaller reductions of primary species than those of secondary species during APEC. Although the contribution of POA to NR-PM_1 showed a rapid decrease as a function of diameter, it still constituted a considerable fraction (~30%) at particle sizes larger than 30 nm. These results suggested that POA played an important role in PM pollution during APEC as a result of large reductions of secondary aerosol.

As indicated in Fig. ~~9~~8, SIA and SOA showed consistently large accumulation modes at ~500–800 nm throughout the day before APEC. This result is consistent with the fact that SIA and SOA were formed mainly over a regional scale and were relatively well processed in the atmosphere. Slight increases in particle diameters in the afternoon were also observed for SIA and SOA, indicating the role of photochemical processing. In contrast, SIA and SOA shifted to smaller sizes at ~300–600 nm at various times of the day during APEC with the mass concentrations above 200 nm showing substantial decreases. As previously discussed, such changes in size and mass during APEC are the combined results of emission controls and meteorological effects. The POA showed significant differences in size evolution behavior from secondary aerosol. The POA size distribution was similar before and during APEC, both characterized by higher concentration at nighttime (19:00 – 3:00) with a peak diameter at ~300 nm. Moreover, a considerable fraction of POA particles was found in ultrafine mode (< 100 nm), particularly in the evening time, indicating local fresh primary emissions. It is worth noting that POA during APEC showed higher mass concentrations between 0:00 and 3:00 than that before APEC~~. This period correlates with that in which no traffic control measures were in place and reflects a~~

~~greater amount of traffic emissions during APEC.~~ , coinciding with a time without traffic control, and likely having more traffic emissions during APEC.

3.5 Elemental composition of OA

Figure ~~10~~ 9 shows the time series of elemental ratios for the entire study period. The O/C ratio, an indicator of the oxidation degree of OA, varied significantly from 0.11 to 0.72, indicating large variations of ~~oxidative~~ oxidation properties of OA in this study. The average O/C for the entire study was 0.41, which is higher than that observed at other urban sites in China , at 0.31–0.33 (He et al., 2011;Huang et al., 2012;Xu et al., 2014;Zhang et al., 2015), yet lower than those measured at rural/remote sites (Huang et al., 2011;Hu et al., 2013). These results indicate that the OA in this study was aged more than that at other urban sites in China. The OM/OC ratio showed similar variations ~~to~~ as those of O/C (R^2 = 0.99), varying between 1.30 and 2.16 with an average value of 1.7 (±0.17). The average OM/OC was slightly higher than the 1.6±0.2 value for urban OA recommended by Turpin and Lim (2001), and the value of 1.6 previously reported in urban Beijing (Huang et al., 2010a;Zhang et al., 2015). The average O/C and OM/OC during APEC were 0.36 (±0.10) and 1.64 (±0.13), respectively, which are lower than 0.43 and 1.75 before APEC , demonstrating a decrease in oxidation degree of OA during APEC . These results are consistent with the OA composition change during APEC, which showed a substantial decrease in SOA and a corresponding increase in POA. Figure ~~10~~ 9 also shows that the O/C ratio exhibited a continuous increase during three severe pollution episodes on October 17–20, October 23–25, and October29–31 with the exception of occasional decreases due to the influences of local POA. These results suggest that OA can be aged to a high degree (O/C > 0.6) during the evolution of severe air pollution. In contrast, such an aging process of OA was observed to be insignificant during APEC.

Both H/C and O/C ratios showed pronounced diurnal cycles before and during APEC (Figs. ~~10e~~9c, d). The O/C ratio showed a gradual increase and reached a maximum value of 0.55 at 16:00 before APEC, indicating the photochemical aging

processes of OA. Such a ~~photo-~~photo-chemical driven diurnal variation of O/C was also observed at various sites in China (He et al., 2011;Xu et al., 2014;Zhang et al., 2015). The O/C also showed a temporal decrease at three times, corresponding to cooking activities. This result indicates that cooking aerosol can significantly influence the bulk oxidation degree of OA. Indeed, the diurnal variation of O/C ratio after excluding COA contributions was markedly smoother, varying from 0.5 to 0.65. The O/C ratio during APEC showed a diurnal pattern similar to that before APEC yet with lower values by ~0.1 throughout the day. This result illustrates that the photochemical aging of OA was significantly less pronounced during APEC. The H/C ratios showed opposite diurnal cycles as those of O/C before and during APEC (Fig. ~~10~~9).

Figure ~~11~~10 shows a Van Krevelen diagram for illustrating the evolution of OA before and during APEC. The aging of OA is generally characterized by an increase in O/C and a decrease in H/C. The different aging mechanisms of OA follow different slopes. Although H/C correlated strongly with O/C before and during APEC (R^2 = 0.84 and 0.81, respectively), the regression slopes differed. The slope of H/C versus O/C during APEC was −0.58 which is steeper than −0.52 measured before APEC. This result indicates their slightly different aging processes mainly driven by the additions of carboxylic acid with fragmentation (Ng et al., 2011). The slope in this study is less than that measured in Changdao at −0.63 (Hu et al., 2013), Shenzhen at −0.87 (He et al., 2011), and Kaiping in PRD at −0.76 (Huang et al., 2011), indicating that the aging mechanism of OA varies among different sites and seasons in China.

As shown in Fig. ~~12a~~11a, The O/C varied dramatically and showed no clear dependence on RH at low RH levels of <60%, although a positive increase as a function of RH before APEC was observed at RH > 60%. These results might indicate that aqueous-phase processing at high RH levels increased the oxidation degree of OA. The POA with high concentration at nighttime when RH is correspondingly high can have a large influence on the O/C of total OA, which explains the slight decrease in O/C as a function of RH during APEC. The O/C ratio of SOA was calculated, and its

relationship with RH is shown in Fig. ~~12b~~11b. It is clear that the O/C ratio of SOA rapidly increased from 0.5 to 0.8 as the RH increased from 10% to >80% before APEC. The O/C of SOA showed similar RH dependence during APEC. Such an increase is mainly caused by a faster increase of LV-OOA than that of SV-OOA. These results likely indicate that aqueous-phase processing produced highly aged OA during the severe haze pollution episodes. However, we found that LV-OOA tightly correlated with NO_3 ($R^2 = 0.94$), whereas aqueous-phase production appeared to play an insignificant role in nitrate formation during winter (Sun et al., 2013). Therefore, the highly aged OA at high RH levels was more likely due to the aging of LV-OOA for a longer time during the transport to Beijing. Further studies are needed to investigate the role of aqueous-phase processing in the alteration of the oxidation properties of OA.

3.6 Case study of the evolution of a severe haze episode

The four-day evolution of a severe pollution episode was observed between October 22 and 25 during which the average PM_1 concentration showed a 10-fold increase from <30μg/m^3 to >300 μg/m^3. As shown in Fig.~~13~~12, this evolution period was characterized by prevailing southerly winds and air masses (Fig. S5), low WS (< 4 m/s) across the entire layer below 500 m, and also relatively high RH (> 50%). Routine circulations of mountain–valley breeze from the northwest and the northeast that occurred at midnight and dissipated at noon were also observed. However, the mountain–valley breeze did not appear to significantly affect the evolution of this haze episode likely because it was a regional haze event with high PM concentration in the entire region of the North China (Fig. S4).

The evolution of this haze episode can be classified into four stages with different aerosol composition and ~~oxidative~~ oxidation properties. The aerosol composition during the early formation stage (~~S1~~E1) was dominated by organics (53%) with a small contribution~~s~~ from SIA (23%). The OA showed dominant contributions from cooking (45%) and traffic (19%) sources, indicating that local sources played the most significant roles during this stage. Consistently, OA showed fresh properties

with an average O/C ratio of 0.25. The aerosol composition had a substantial change during stage 2 (~~S2~~E2). Although the contribution of organics decreased to 41%, those of sulfate and nitrate increased nearly by a factor of two (10% and 19%, respectively). The O/C ratio of OA increased from ~0.2 to ~0.5, suggesting the occurrence of more aged air masses during ~~S2~~E2. Indeed, the contribution of LV-OOA showed a great enhancement from 6% to 19%, whereas that of SV-OOA exhibited minor changes. As this haze episode progressed (stage 3, ~~S3~~E3), ~~the~~ SIA exceeded ~~the~~ organics and became the dominant component in PM_1 (53%); in particular, nitrate accounted for nearly one-third of the total PM_1 mass. These results highlight the enhanced roles of SIA in severe haze episodes, which ~~is~~ are consistent with the conclusions drawn in many previous studies in China (Huang et al., 2014;Sun et al., 2014). OA was further aged during this stage with the O/C ratio approaching 0.6, and the highly oxidized LV-OOA accounting for nearly one-third of the total OA. The haze episode evolved further at 10:00 on October 24 with a large enhancement of PM_1 from ~150 μg/m^3 to > 200 μg/m^3, which remained consistently high for 1.5 days (stage 4, ~~S4~~E4). The aerosol composition during this stage remained relatively constant. SIA contributed more than 60% of the total PM_1, and SOA accounted for 67% of the total OA, which together contributed 82% of the total PM_1, further elucidating the significant role of secondary aerosol in haze formation.

Although SIA was observed to gradually increase during the evolution of this haze episode, primary aerosol species such as COA, HOA, and BC showed similar diurnal variations during ~~S3~~ E3 and ~~S4~~E4, indicating relatively constant local emissions during these two stages. Although the daily maximum of O/C showed a continuous increase, pronounced diurnal cycles with the lowest values occurring at mid-night were also observed due to the influences of local primary OA. The O/C of SOA was then calculated for a better illustration of OA aging. As shown in Fig. ~~13d~~12d, the O/C ratio of SOA showed a gradual increase from ~0.55 to 0.8 during ~~S1~~E1–~~S3~~ E3 and remained consistently high (~0.8) during ~~S4~~E4. This result is consistent with the relative contributions of LV-OOA and SV-OOA during the four

evolution stages. Although SV-OOA was higher than LV-OOA during ~~S1~~E1, LV-OOA gradually exceeded SV-OOA and became the dominant contributor of OA during the following three stages. These results illustrate that the aging of the haze episode was associated with significant formation of highly oxidized OA. The Van Krevelen diagram of H/C versus O/C for this haze episode is shown in Fig. ~~11~~10. It is clear that OA evolved rapidly during this haze episode, showing an increase in O/C associated with a corresponding decrease in H/C with a slope of −0.6.

Figure ~~14~~13 shows the evolution of size distributions of sulfate, nitrate, and organics during this haze episode. Sulfate and nitrate showed evident particle growth as a function of time. Although broad size distributions peaking at ~350 nm were observed during ~~S1~~E1, the peak diameters gradually evolved to ~700 nm during ~~S4~~E4; these size distributions were characterized by single large accumulation modes. Organics showed similar size evolution behavior as that of sulfate and nitrate but presented significant contributions from particles smaller than 200 nm. In particular, the influences of local primary emissions such as cooking and traffic on small particles were observed at nighttime during October 23–25. Overall, the aerosol composition, ~~oxidative~~ oxidation properties, and size distributions exhibited substantial changes during the evolution of the severe haze episode, which was characterized by the significant enhancement of SIA and SOA with high oxidation degrees and large particle diameters.

4. Conclusions

China imposed strict emission controls in Beijing and its surrounding regions during the 2014 APEC summit. In this study, we present a detailed investigation of the impacts of emission controls on the changes in chemical composition, ~~oxidative~~ oxidation properties, and size distributions of submicron aerosols. The average mass concentration of PM_1 showed a substantial decrease from 88.0 μg/m^3 before APEC to 41.6 μg/m^3 during APEC. The aerosol composition also showed significant changes. Although submicron aerosols were composed mainly of organics, at 38.0%, followed by nitrate at 26.4% and sulfate at 13.7% before APEC, the contribution of organics

was observed to have a significant increase at 52.4% associated with ~~the~~ a significant reduction~~s~~ of SIA during APEC. This result demonstrates the different responses of SIA and OA to regional emission controls. PMF analysis of OA identified three primary sources ~~such as~~ including traffic, cooking, and biomass burning emissions and two secondary factors with different oxidation degrees. The highly oxidized LV-OOA showed reductions similar to those of SIA with the contribution to OA decreasing from 30% to 14%. In contrast, POA showed elevated contributions indicating the presence of strong local source emissions during APEC. The O/C ratio of OA decreased from 0.43 to 0.36, demonstrating a decrease in the oxidization degree of OA during APEC. The peak diameters in size distributions of SIA and SOA were ~650nm or even larger before APEC and shifted to smaller sizes of ~400 nm during APEC. This result illustrates that emission controls of secondary aerosol precursors exerted a dominant impact in reducing accumulation mode particles. Comparatively, the size distributions of POA remained relatively unchanged. Therefore, our results elucidated significant changes in chemical composition, size distributions, and ~~oxidative~~ oxidation properties of aerosol particles as a result of emission controls and meteorological effects. In addition, we observed significant changes in aerosol properties during the aging processes of a severe haze pollution episode, which was typically characterized by a gradual increase of SIA and SOA with higher oxidation degrees and large particle diameters. Note that the routine circulation of a mountain–valley breeze during APEC was also observed to play a role in achieving "APEC blue" by conditions reducing PM levels substantially during daytime. Despite the fact that controlling secondary aerosol precursors over regional scales can substantially reduce secondary particulates, stricter controls of local source emissions are needed for further mitigation of air pollution in Beijing.

Acknowledgements

This work was supported by the National Key Project of Basic Research (2014CB447900), the Strategic Priority Research Program (B) of the Chinese Academy of Sciences (XDB05020501), the Key Research Program of the Chinese

747 Academy of Sciences (KJZD-EW-TZ-G06-01-0), and the Special Fund for
748 Environmental Protection Research in the Public Interest (201409001).

749

750 **References**

751 Aiken, A. C., DeCarlo, P. F., and Jimenez, J. L.: Elemental analysis of organic species
752 with electron ionization high-resolution mass spectrometry, Anal. Chem., 79,
753 8350-8358, 2007.
754 Aiken, A. C., Salcedo, D., Cubison, M. J., Huffman, J. A., DeCarlo, P. F., Ulbrich, I.
755 M., Docherty, K. S., Sueper, D., Kimmel, J. R., Worsnop, D. R., Trimborn, A.,
756 Northway, M., Stone, E. A., Schauer, J. J., Volkamer, R. M., Fortner, E., de Foy,
757 B., Wang, J., Laskin, A., Shutthanandan, V., Zheng, J., Zhang, R., Gaffney, J.,
758 Marley, N. A., Paredes-Miranda, G., Arnott, W. P., Molina, L. T., Sosa, G., and
759 Jimenez, J. L.: Mexico City aerosol analysis during MILAGRO using high
760 resolution aerosol mass spectrometry at the urban supersite (T0) - Part 1: Fine
761 particle composition and organic source apportionment, Atmos. Chem. Phys., 9,
762 6633-6653, 2009.
763 Alfarra, M. R., Prevot, A. S. H., Szidat, S., Sandradewi, J., Weimer, S., Lanz, V. A.,
764 Schreiber, D., Mohr, M., and Baltensperger, U.: Identification of the mass
765 spectral signature of organic aerosols from wood burning emissions, Environ. Sci.
766 Technol., 41, 5770-5777, 2007.
767 Allan, J. D., Jimenez, J. L., Williams, P. I., Alfarra, M. R., Bower, K. N., Jayne, J. T.,
768 Coe, H., and Worsnop, D. R.: Quantitative sampling using an Aerodyne Aerosol
769 Mass Spectrometer. Part 1: Techniques of data interpretation and error analysis, J.
770 Geophys. Res.-Atmos., 108, 4090, doi:4010.1029/2002JD002358, 2003.
771 Canagaratna, M. R., Jimenez, J. L., Kroll, J. H., Chen, Q., Kessler, S. H., Massoli, P.,
772 Hildebrandt Ruiz, L., Fortner, E., Williams, L. R., Wilson, K. R., Surratt, J. D.,
773 Donahue, N. M., Jayne, J. T., and Worsnop, D. R.: Elemental ratio measurements
774 of organic compounds using aerosol mass spectrometry: characterization,
775 improved calibration, and implications, Atmos. Chem. Phys., 15, 253-272,
776 10.5194/acp-15-253-2015, 2015.
777 Cao, J. J., Wu, F., Chow, J. C., Lee, S. C., Li, Y., Chen, S. W., An, Z. S., Fung, K. K.,
778 Watson, J. G., Zhu, C. S., and Liu, S. X.: Characterization and source
779 apportionment of atmospheric organic and elemental carbon during fall and
780 winter of 2003 in Xi'an, China, Atmos. Chem. Phys., 5, 3127-3137,
781 10.5194/acp-5-3127-2005, 2005.
782 Cermak, J., and Knutti, R.: Beijing Olympics as an aerosol field experiment, Geophys.
783 Res. Lett., 36, 10.1029/2009gl038572, 2009.
784 Chen, C., Sun, Y. L., Xu, W. Q., Du, W., Zhou, L. B., Han, T. T., Wang, Q. Q., Fu, P.
785 Q., Wang, Z. F., Gao, Z. Q., Zhang, Q., and Worsnop, D. R.: Characteristics and
786 sources of submicron aerosols above the urban canopy (260 m) in Beijing, China
787 during 2014 APEC summit, Atmos. Chem. Phys. Discuss., 15, 22889-22934,
788 10.5194/acpd-15-22889-2015, 2015.

789 Chow, J. C., Bachmann, J. D., Wierman, S. S. G., Mathai, C. V., Malm, W. C., White,
790 W. H., Mueller, P. K., Kumar, N., and Watson, J. G.: Visibility: Science and
791 Regulation, J. Air Waste Manage. Assoc., 52, 973-999,
792 10.1080/10473289.2002.10470844, 2002.
793 Cubison, M. J., Ortega, A. M., Hayes, P. L., Farmer, D. K., Day, D., Lechner, M. J.,
794 Brune, W. H., Apel, E., Diskin, G. S., Fisher, J. A., Fuelberg, H. E., Hecobian, A.,
795 Knapp, D. J., Mikoviny, T., Riemer, D., Sachse, G. W., Sessions, W., Weber, R. J.,
796 Weinheimer, A. J., Wisthaler, A., and Jimenez, J. L.: Effects of aging on organic
797 aerosol from open biomass burning smoke in aircraft and laboratory studies,
798 Atmos. Chem. Phys., 11, 12049-12064, 10.5194/acp-11-12049-2011, 2011.
799 Dan, M., Zhuang, G., Li, X., Tao, H., and Zhuang, Y.: The characteristics of
800 carbonaceous species and their sources in PM2.5 in Beijing, Atmos. Environ., 38,
801 3443-3452, 2004.
802 DeCarlo, P. F., Kimmel, J. R., Trimborn, A., Northway, M. J., Jayne, J. T., Aiken, A.
803 C., Gonin, M., Fuhrer, K., Horvath, T., Docherty, K. S., Worsnop, D. R., and
804 Jimenez, J. L.: Field-Deployable, High-Resolution, Time-of-Flight Aerosol Mass
805 Spectrometer, Anal. Chem., 78, 8281-8289, 2006.
806 DeCarlo, P. F., Ulbrich, I. M., Crounse, J., de Foy, B., Dunlea, E. J., Aiken, A. C.,
807 Knapp, D., Weinheimer, A. J., Campos, T., Wennberg, P. O., and Jimenez, J. L.:
808 Investigation of the sources and processing of organic aerosol over the Central
809 Mexican Plateau from aircraft measurements during MILAGRO, Atmos. Chem.
810 Phys., 10, 5257-5280, 10.5194/acp-10-5257-2010, 2010.
811 Drewnick, F., Hings, S. S., DeCarlo, P., Jayne, J. T., Gonin, M., Fuhrer, K., Weimer, S.,
812 Jimenez, J. L., Demerjian, K. L., Borrmann, S., and Worsnop, D. R.: A New
813 Time-of-Flight Aerosol Mass Spectrometer (TOF-AMS)—Instrument
814 Description and First Field Deployment, Aerosol Sci. Tech., 39, 637-658,
815 10.1080/02786820500182040, 2005.
816 Forster, P., Ramaswamy, V., Artaxo, P., Berntsen, T., Betts, R., Fahey, D. W.,
817 Haywood, J., Lean, J., Lowe, D. C., Myhre, G., Nganga, J., Prinn, R., Raga, G.,
818 Schulz, M., and Dorland, R. V.: Changes in Atmospheric Constituents and in
819 Radiative Forcing., in: Climate Change 2007: The Physical Science Basis.
820 Contribution of Working Group I to the Fourth Assessment Report of the
821 Intergovernmental Panel on Climate Change, edited by: Solomon, S., D. Qin, M.
822 Manning, Z. Chen, M. Marquis, K.B. Averyt, M.Tignor and H.L. Miller,
823 Cambridge University Press, Cambridge, United Kingdom and New York, NY,
824 USA., 2007.
825 Ge, X., Setyan, A., Sun, Y., and Zhang, Q.: Primary and secondary organic aerosols in
826 Fresno, California during wintertime: Results from high resolution aerosol mass
827 spectrometry, J. Geophys. Res., 117, D19301, 10.1029/2012JD018026, 2012a.
828 Ge, X., Zhang, Q., Sun, Y., Ruehl, C. R., and Setyan, A.: Effect of aqueous-phase
829 processing on aerosol chemistry and size distributions in Fresno, California,
830 during wintertime, Environmental Chemistry, 9, 221, 10.1071/en11168, 2012b.
831 Guo, S., Hu, M., Guo, Q., Zhang, X., Zheng, M., Zheng, J., Chang, C.-C., Schauer, J.
832 J., and Zhang, R.: Primary Sources and Secondary Formation of Organic

Aerosols in Beijing, China, Environ. Sci. Technol., 10.1021/es2042564, 2012.
Guo, S., Hu, M., Guo, Q., Zhang, X., Schauer, J. J., and Zhang, R.: Quantitative evaluation of emission controls on primary and secondary organic aerosol sources during Beijing 2008 Olympics, Atmos. Chem. Phys., 13, 8303-8314, 10.5194/acp-13-8303-2013, 2013.
Han, S., Kondo, Y., Oshima, N., Takegawa, N., Miyazaki, Y., Hu, M., Lin, P., Deng, Z., Zhao, Y., Sugimoto, N., and Wu, Y.: Temporal variations of elemental carbon in Beijing, J. Geophys. Res., 114, 10.1029/2009jd012027, 2009.
He, L.-Y., Huang, X.-F., Xue, L., Hu, M., Lin, Y., Zheng, J., Zhang, R., and Zhang, Y.-H.: Submicron aerosol analysis and organic source apportionment in an urban atmosphere in Pearl River Delta of China using high-resolution aerosol mass spectrometry, J. Geophys. Res., 116, D12304, 10.1029/2010jd014566, 2011.
He, L. Y., Lin, Y., Huang, X. F., Guo, S., Xue, L., Su, Q., Hu, M., Luan, S. J., and Zhang, Y. H.: Characterization of high-resolution aerosol mass spectra of primary organic aerosol emissions from Chinese cooking and biomass burning, Atmos. Chem. Phys., 10, 11535-11543, 10.5194/acp-10-11535-2010, 2010.
Heald, C. L., Kroll, J. H., Jimenez, J. L., Docherty, K. S., DeCarlo, P. F., Aiken, A. C., Chen, Q., Martin, S. T., Farmer, D. K., and Artaxo, P.: A simplified description of the evolution of organic aerosol composition in the atmosphere, Geophys. Res. Lett., 37, L08803, 10.1029/2010gl042737, 2010.
Hu, W. W., Hu, M., Yuan, B., Jimenez, J. L., Tang, Q., Peng, J. F., Hu, W., Shao, M., Wang, M., Zeng, L. M., Wu, Y. S., Gong, Z. H., Huang, X. F., and He, L. Y.: Insights on organic aerosol aging and the influence of coal combustion at a regional receptor site of central eastern China, Atmos. Chem. Phys., 13, 10095-10112, 10.5194/acp-13-10095-2013, 2013.
Huang, R. J., Zhang, Y., Bozzetti, C., Ho, K. F., Cao, J. J., Han, Y., Daellenbach, K. R., Slowik, J. G., Platt, S. M., Canonaco, F., Zotter, P., Wolf, R., Pieber, S. M., Bruns, E. A., Crippa, M., Ciarelli, G., Piazzalunga, A., Schwikowski, M., Abbaszade, G., Schnelle-Kreis, J., Zimmermann, R., An, Z., Szidat, S., Baltensperger, U., El Haddad, I., and Prevot, A. S.: High secondary aerosol contribution to particulate pollution during haze events in China, Nature, 514, 218-222, 10.1038/nature13774, 2014.
Huang, X.-F., Xue, L., Tian, X.-D., Shao, W.-W., Sun, T.-L., Gong, Z.-H., Ju, W.-W., Jiang, B., Hu, M., and He, L.-Y.: Highly time-resolved carbonaceous aerosol characterization in Yangtze River Delta of China: Composition, mixing state and secondary formation, Atmos. Environ., 64, 200-207, 10.1016/j.atmosenv.2012.09.059, 2013.
Huang, X., Xue, L., He, L., Hu, M., Zhang, Y., and Zhu, T.: On-line measurement of organic aerosol elemental composition based on high resolution aerosol mass spectrometry, Chin. Sci. Bull., 55, 3391-3396, 10.1360/972010-1322, 2010a.
Huang, X. F., He, L. Y., Hu, M., Canagaratna, M. R., Sun, Y., Zhang, Q., Zhu, T., Xue, L., Zeng, L. W., Liu, X. G., Zhang, Y. H., Jayne, J. T., Ng, N. L., and Worsnop, D. R.: Highly time-resolved chemical characterization of atmospheric submicron particles during 2008 Beijing Olympic Games using an Aerodyne

High-Resolution Aerosol Mass Spectrometer, Atmos. Chem. Phys., 10, 8933-8945, 10.5194/acp-10-8933-2010, 2010b.

Huang, X. F., He, L. Y., Hu, M., Canagaratna, M. R., Kroll, J. H., Ng, N. L., Zhang, Y. H., Lin, Y., Xue, L., Sun, T. L., Liu, X. G., Shao, M., Jayne, J. T., and Worsnop, D. R.: Characterization of submicron aerosols at a rural site in Pearl River Delta of China using an Aerodyne High-Resolution Aerosol Mass Spectrometer, Atmos. Chem. Phys., 11, 1865-1877, 10.5194/acp-11-1865-2011, 2011.

Huang, X. F., He, L. Y., Xue, L., Sun, T. L., Zeng, L. W., Gong, Z. H., Hu, M., and Zhu, T.: Highly time-resolved chemical characterization of atmospheric fine particles during 2010 Shanghai World Expo, Atmos. Chem. Phys., 12, 4897-4907, 10.5194/acp-12-4897-2012, 2012.

Jayne, J. T., Leard, D. C., Zhang, X., Davidovits, P., Smith, K. A., Kolb, C. E., and Worsnop, D. R.: Development of an aerosol mass spectrometer for size and composition analysis of submicron particles, Aerosol Sci. Tech., 33, 49-70, 2000.

Jimenez, J. L.: Ambient aerosol sampling using the Aerodyne Aerosol Mass Spectrometer, J. Geophys. Res., 108, 10.1029/2001jd001213, 2003.

Kroll, J. H., Donahue, N. M., Jimenez, J. L., Kessler, S. H., Canagaratna, M. R., Wilson, K. R., Altieri, K. E., Mazzoleni, L. R., Wozniak, A. S., Bluhm, H., Mysak, E. R., Smith, J. D., Kolb, C. E., and Worsnop, D. R.: Carbon oxidation state as a metric for describing the chemistry of atmospheric organic aerosol, Nature Chemistry, 3, 133-139, doi:10.1038/nchem.948, 2011.

Lee, B. P., Li, Y. J., Yu, J. Z., Louie, P. K. K., and Chan, C. K.: Physical and chemical characterization of ambient aerosol by HR-ToF-AMS at a suburban site in Hong Kong during springtime 2011, Journal of Geophysical Research: Atmospheres, 118, 8625-8639, 10.1002/jgrd.50658, 2013.

Levin, E. J. T., McMeeking, G. R., Carrico, C. M., Mack, L. E., Kreidenweis, S. M., Wold, C. E., Moosmüller, H., Arnott, W. P., Hao, W. M., Collett, J. L., Jr., and Malm, W. C.: Biomass burning smoke aerosol properties measured during Fire Laboratory at Missoula Experiments (FLAME), J. Geophys. Res., 115, D18210, 10.1029/2009jd013601, 2010.

Matthew, B. M., Middlebrook, A. M., and Onasch, T. B.: Collection Efficiencies in an Aerodyne Aerosol Mass Spectrometer as a Function of Particle Phase for Laboratory Generated Aerosols, Aerosol Sci. Tech., 42, 884-898, 10.1080/02786820802356797, 2008.

Middlebrook, A. M., Bahreini, R., Jimenez, J. L., and Canagaratna, M. R.: Evaluation of Composition-Dependent Collection Efficiencies for the Aerodyne Aerosol Mass Spectrometer using Field Data, Aerosol Sci. Tech., 46, 258-271, 10.1080/02786826.2011.620041, 2012.

Mohr, C., Huffman, J. A., Cubison, M. J., Aiken, A. C., Docherty, K. S., Kimmel, J. R., Ulbrich, I. M., Hannigan, M., and Jimenez, J. L.: Characterization of primary organic aerosol emissions from meat cooking, trash burning, and motor vehicles with High-Resolution Aerosol Mass Spectrometry and comparison with ambient and chamber observations, Environ. Sci. Technol., 43, 2443-2449, doi:10.1021/es8011518, 2009.

Ng, N. L., Canagaratna, M. R., Jimenez, J. L., Chhabra, P. S., Seinfeld, J. H., and Worsnop, D. R.: Changes in organic aerosol composition with aging inferred from aerosol mass spectra, Atmos. Chem. Phys., 11, 6465-6474, 10.5194/acp-11-6465-2011, 2011.

Paatero, P., and Tapper, U.: Positive matrix factorization: A non-negative factor model with optimal utilization of error estimates of data values, Environmetrics, 5, 111-126, 1994.

Pope, C. A., III, Ezzati, M., and Dockery, D. W.: Fine-Particulate Air Pollution and Life Expectancy in the United States, New England Journal of Medicine, 360, 376-386, 10.1056/NEJMsa0805646, 2009.

Shao, M., Wang, B., Lu, S., Yuan, B., and Wang, M.: Effects of Beijing Olympics Control Measures on Reducing Reactive Hydrocarbon Species, Environ. Sci. Technol., 45, 514-519, 10.1021/es102357t, 2011.

Song, Y., Zhang, Y., Xie, S., Zeng, L., Zheng, M., Salmon, L. G., Shao, M., and Slanina, S.: Source apportionment of PM2.5 in Beijing by positive matrix factorization, Atmos. Environ., 40, 1526-1537, DOI: 10.1016/j.atmosenv.2005.10.039, 2006.

Sun, J., Zhang, Q., Canagaratna, M. R., Zhang, Y., Ng, N. L., Sun, Y., Jayne, J. T., Zhang, X., Zhang, X., and Worsnop, D. R.: Highly time- and size-resolved characterization of submicron aerosol particles in Beijing using an Aerodyne Aerosol Mass Spectrometer, Atmos. Environ., 44, 131-140, 10.1016/j.atmosenv.2009.03.020, 2010.

Sun, Y., Wang, Z., Dong, H., Yang, T., Li, J., Pan, X., Chen, P., and Jayne, J. T.: Characterization of summer organic and inorganic aerosols in Beijing, China with an Aerosol Chemical Speciation Monitor, Atmos. Environ., 51, 250-259, 10.1016/j.atmosenv.2012.01.013, 2012.

Sun, Y., Jiang, Q., Wang, Z., Fu, P., Li, J., Yang, T., and Yin, Y.: Investigation of the sources and evolution processes of severe haze pollution in Beijing in January 2013, J. Geophys. Res.-Atmos., 119, 4380-4398, 10.1002/2014jd021641, 2014.

Sun, Y. L., Zhang, Q., Schwab, J. J., Chen, W. N., Bae, M. S., Hung, H. M., Lin, Y. C., Ng, N. L., Jayne, J., Massoli, P., Williams, L. R., and Demerjian, K. L.: Characterization of near-highway submicron aerosols in New York City with a high-resolution time-of-flight aerosol mass spectrometer, Atmos. Chem. Phys. Discuss., 11, 30719-30755, 10.5194/acpd-11-30719-2011, 2011a.

Sun, Y. L., Zhang, Q., Schwab, J. J., Demerjian, K. L., Chen, W. N., Bae, M. S., Hung, H. M., Hogrefe, O., Frank, B., Rattigan, O. V., and Lin, Y. C.: Characterization of the sources and processes of organic and inorganic aerosols in New York City with a high-resolution time-of-flight aerosol mass spectrometer, Atmos. Chem. Phys., 11, 1581-1602, 10.5194/acp-11-1581-2011, 2011b.

Sun, Y. L., Wang, Z. F., Fu, P. Q., Yang, T., Jiang, Q., Dong, H. B., Li, J., and Jia, J. J.: Aerosol composition, sources and processes during wintertime in Beijing, China, Atmos. Chem. Phys., 13, 4577-4592, 10.5194/acp-13-4577-2013, 2013.

Takegawa, N., Miyakawa, T., Watanabe, M., Kondo, Y., Miyazaki, Y., Han, S., Zhao, Y., van Pinxteren, D., Bruggemann, E., Gnauk, T., Herrmann, H., Xiao, R., Deng,

965 Z., Hu, M., Zhu, T., and Zhang, Y.: Performance of an Aerodyne Aerosol Mass
966 Spectrometer (AMS) during Intensive Campaigns in China in the Summer of
967 2006, Aerosol Sci. Tech., 43, 189-204, 10.1080/02786820802582251, 2009.
968 Ulbrich, I. M., Canagaratna, M. R., Zhang, Q., Worsnop, D. R., and Jimenez, J. L.:
969 Interpretation of organic components from Positive Matrix Factorization of
970 aerosol mass spectrometric data, Atmos. Chem. Phys., 9, 2891-2918, 2009.
971 Wang, H., Zhuang, Y., Wang, Y., Sun, Y., Yuan, H., Zhuang, G., and Hao, Z.:
972 Long-term monitoring and source apportionment of PM2.5/PM10 in Beijing,
973 China, Journal of Environmental Sciences, 20, 1323-1327, 2008.
974 Wang, T., Nie, W., Gao, J., Xue, L. K., Gao, X. M., Wang, X. F., Qiu, J., Poon, C. N.,
975 Meinardi, S., Blake, D., Wang, S. L., Ding, A. J., Chai, F. H., Zhang, Q. Z., and
976 Wang, W. X.: Air quality during the 2008 Beijing Olympics: secondary
977 pollutants and regional impact, Atmos. Chem. Phys., 10, 7603-7615,
978 10.5194/acp-10-7603-2010, 2010.
979 Wang, W., Primbs, T., Tao, S., and Simonich, S. L. M.: Atmospheric Particulate
980 Matter Pollution during the 2008 Beijing Olympics, Environ. Sci. Technol., 43,
981 5314-5320, 10.1021/es9007504, 2009.
982 Wang, W., Jariyasopit, N., Schrlau, J., Jia, Y., Tao, S., Yu, T.-W., Dashwood, R. H.,
983 Zhang, W., Wang, X., and Simonich, S. L. M.: Concentration and
984 Photochemistry of PAHs, NPAHs, and OPAHs and Toxicity of PM2.5 during the
985 Beijing Olympic Games, Environ. Sci. Technol., 45, 6887-6895,
986 10.1021/es201443z, 2011.
987 Xu, J., Zhang, Q., Chen, M., Ge, X., Ren, J., and Qin, D.: Chemical composition,
988 sources, and processes of urban aerosols during summertime in northwest China:
989 insights from high-resolution aerosol mass spectrometry, Atmos. Chem. Phys.,
990 14, 12593-12611, 10.5194/acp-14-12593-2014, 2014.
991 Zhang, H., Wang, S., Hao, J., Wan, L., Jiang, J., Zhang, M., Mestl, H. E. S., Alnes, L.
992 W. H., Aunan, K., and Mellouki, A. W.: Chemical and size characterization of
993 particles emitted from the burning of coal and wood in rural households in
994 Guizhou, China, Atmos. Environ., 51, 94-99, 10.1016/j.atmosenv.2012.01.042,
995 2012a.
996 Zhang, J., Wang, Y., Huang, X., Liu, Z., Ji, D., and Sun, Y.: Characterization of
997 organic aerosols in Beijing using an aerodyne high-resolution aerosol mass
998 spectrometer, Advances in Atmospheric Sciences, 32, 877-888,
999 10.1007/s00376-014-4153-9, 2015.
1000 Zhang, J. K., Sun, Y., Liu, Z. R., Ji, D. S., Hu, B., Liu, Q., and Wang, Y. S.:
1001 Characterization of submicron aerosols during a month of serious pollution in
1002 Beijing, 2013, Atmos. Chem. Phys., 14, 2887-2903, 10.5194/acp-14-2887-2014,
1003 2014a.
1004 Zhang, Q., Worsnop, D. R., Canagaratna, M. R., and Jimenez, J. L.: Hydrocarbon-like
1005 and oxygenated organic aerosols in Pittsburgh: Insights into sources and
1006 processes of organic aerosols, Atmos. Chem. Phys., 5, 3289-3311, 2005.
1007 Zhang, Q., Jimenez, J. L., Worsnop, D. R., and Canagaratna, M.: A case study of
1008 urban particle acidity and its effect on secondary organic aerosol, Environ. Sci.

Technol., 41, 3213-3219, 2007.
Zhang, Q. H., Zhang, J. P., and Xue, H. W.: The challenge of improving visibility in Beijing, Atmos. Chem. Phys., 10, 7821-7827, 10.5194/acp-10-7821-2010, 2010.
Zhang, R., Jing, J., Tao, J., Hsu, S. C., Wang, G., Cao, J., Lee, C. S. L., Zhu, L., Chen, Z., Zhao, Y., and Shen, Z.: Chemical characterization and source apportionment of PM2.5 in Beijing: seasonal perspective, Atmos. Chem. Phys., 13, 7053-7074, 10.5194/acp-13-7053-2013, 2013.
Zhang, Y., Sun, J., Zhang, X., Shen, X., Wang, T., and Qin, M.: Seasonal characterization of components and size distributions for submicron aerosols in Beijing, Science China Earth Sciences, 56, 890-900, 10.1007/s11430-012-4515-z, 2012b.
Zhang, Y. M., Zhang, X. Y., Sun, J. Y., Hu, G. Y., Shen, X. J., Wang, Y. Q., Wang, T. T., Wang, D. Z., and Zhao, Y.: Chemical composition and mass size distribution of PM1 at an elevated site in central east China, Atmos. Chem. Phys., 14, 12237-12249, 10.5194/acp-14-12237-2014, 2014b.
Zheng, G. J., Duan, F. K., Su, H., Ma, Y. L., Cheng, Y., Zheng, B., Zhang, Q., Huang, T., Kimoto, T., Chang, D., Pöschl, U., Cheng, Y. F., and He, K. B.: Exploring the severe winter haze in Beijing: the impact of synoptic weather, regional transport and heterogeneous reactions, Atmos. Chem. Phys., 15, 2969-2983, 10.5194/acp-15-2969-2015, 2015.
Zheng, M., Salmon, L. G., Schauer, J. J., Zeng, L., Kiang, C. S., Zhang, Y., and Cass, G. R.: Seasonal trends in PM2.5 source contributions in Beijing, China, Atmos. Environ., 39, 3967-3976, DOI: 10.1016/j.atmosenv.2005.03.036, 2005.

Table1. Summary of average meteorological parameters, mass concentrations of PM_1 Species and OA factors for the entire study, before and during APEC, and also the change percentages during APEC.

	Entire Study	Before APEC	APEC	Change Perc. (%)
Meteorological Parameters				
RH(%)	47.5	52.8	37.4	
T(°C)	13.0	14.5	10.1	
PM_1 Species (μg/m^3)				
Org	29.4	33.6	21.8	35.1
SO_4	9.1	12.0	3.7	69.2
NO_3	17.8	23.1	7.7	66.7
NH_4	7.8	9.8	3.7	62.2
Chl	2.9	3.4	2.0	41.2
BC	4.8	6.1	2.7	55.7
PM_1	71.8	88.0	41.6	52.7
OA (μg/m^3)				
COA1	5.5	5.9	4.7	20.3
COA2	2.0	2.2	1.6	27.3
HOA	3.4	3.6	2.9	19.4
BBOA	4.1	4.3	3.6	16.3
SV-OOA	7.0	8.6	3.8	55.8
LV-OOA	7.9	10.6	2.8	73.6

Figure captions:

Figure~~Fig.~~ 1. Time series of (a) relative humidity (RH), temperature (*T*), (b) wind direction (WD), wind speed (WS), (c) mass concentrations, and (d) mass fractions of chemical species in PM_1. The pie charts show the average chemical composition of PM_1 measured before and during the Asia–Pacific Economic Cooperation (APEC) summit.

~~**Fig. 2.** Correlation between predicted NH_4^+ and measured NH_4^+ recorded before and during the Asia–Pacific Economic Cooperation (APEC) summit.~~

Figure~~Fig.~~ ~~3~~2. Diurnal profiles of the mass concentrations of PM_1 species measured before and during the Asia–Pacific Economic Cooperation (APEC) summit. Also shown are the changes in percentage of aerosol species occurring during APEC.

~~**Fig. 4.** Diurnal evolution of the composition of PM_1 and organic aerosols (OA) measured (a), (c) before the Asia–Pacific Economic Cooperation summit (APEC) and (b), (d) during APEC.~~

Figure~~Fig.~~ ~~5~~3. High-resolution mass spectra (HRMS; left panel) and time series (right panel) of six organic aerosols (OA) components (a) hydrocarbon-like aerosol (HOA), (b) biomass burning OA (BBOA), (c) cooking organic aerosol 2 (COA2), (d) COA1, (e) semi-volatile oxygenated OA (SV-OOA), and (f) low-volatility oxygenated OA (LV-OOA). Also shown in the right panel are the time series of ~~external~~ tracers including $C_6H_{10}O^+$, $C_2H_4O_2^+$, CO, black carbon (BC), nitrate and ~~SNA~~ SIA (sulfate + nitrate + ammonium). The two pie charts show the average chemical composition of PM_1 measured before and during the Asia–Pacific Economic Cooperation (APEC) summit, respectively. The correlation coefficients between OA factors and external tracers measured before and during APEC are also shown in the figure.

Figure 4. Diurnal evolution of the composition of PM_1 and organic aerosols (OA) measured (a), (c) before the Asia–Pacific Economic Cooperation summit (APEC) and (b), (d) during APEC.

Figure~~Fig.~~ ~~6~~5. Diurnal profiles of the mass concentrations of organic aerosol (OA) factors measured before and during the Asia–Pacific Economic Cooperation (APEC)

summit. Also shown are the changes in percentage of OA factors measured during APEC.

Figure~~Fig. 7~~6. Relative humidity (RH) and wind dependence (WD) of (a), (b) semi-volatile oxygenated organic aerosols (SV-OOA), (c), (d) low-volatility oxygenated organic aerosols (LV-OOA), and (e), (f) the ratio of LV-OOA/SV-OOA measured before (left panel) and during the Asia–Pacific Economic Cooperation (APEC) summit (right panel). S refers to the south (90° < WD < 270°), and N refers to the north (0°< WD < 90° and 270° < WD < 360°). Grids with points numbering less than five were excluded.

Figure~~Fig. 8~~7. Average size distributions and fractions of NR-PM_1 species, primary organic aerosols (POA) and oxygenated organic aerosols (OOA) measured (a) before the Asia–Pacific Economic Cooperation (APEC) summit and (b) during APEC.

Figure~~Fig~~ ~~9~~8. Diurnal evolution of the size distributions of NR-PM_1 species measured (a) before the Asia–Pacific Economic Cooperation (APEC) and (b) during APEC.

Figure~~Fig. 10~~ 9. Time series of (a) H/C, (b) O/C, and organics, and diurnal variations of (c) O/C and (d) H/C. The dashed lines in (c) and (d) indicate the elemental ratios by excluding the contributions from cooking aerosols.

Figure~~Fig.11~~10. Van Krevelen diagram of H/C versus O/C. The dashed lines indicate changes in H/C against O/C due to the addition of specific functional groups to aliphatic carbon (Heald et al., 2010). The pink and blue lines are derived from the right and left lines in the triangle plot of positive matrix factors (PMF) determined from 43 sites in the Northern Hemisphere (Ng et al., 2011). The color-coded H/C versus O/C refers to the data measured during the severe haze episode shown in Fig. ~~13~~12.

Figure~~Fig. 12~~11. Variations in (a) O/C and (b) O/C of secondary organic aerosols (SOA) as a function of relative humidity (RH) measured (a) before the Asia–Pacific Economic Cooperation (APEC) summit and (b) during APEC. The data are also binned according to RH with increments of 10%.

Figure~~Fig.~~ ~~13~~12. Evolution of meteorological variables including (a)–(c) relative humidity (RH), temperature (*T*), and vertical profiles of wind direction (WD) and wind speed (WS); (d) O/C and O/C of secondary organic aerosols (SOA); (e) organic aerosol (OA) factors; and (f) PM_1 species. The pie charts show the average chemical composition of PM_1 and OA for each stage. The numbers on the pie charts show the contributions of (e) semi-volatile oxygenated organic aerosols (SV-OOA) and low-volatility oxygenated organic aerosols (LV-OOA) and (f) organics, nitrate, and sulfate.

Figure~~Fig.~~ ~~14~~13. (a) Evolution of size distributions of sulfate, nitrate, and organics during the severe haze episode between October 22 and 25 (Fig.12). (b) Average size distributions of sulfate, nitrate, and organics during the four stages of E1-E4. ~~these three species for each stage.~~

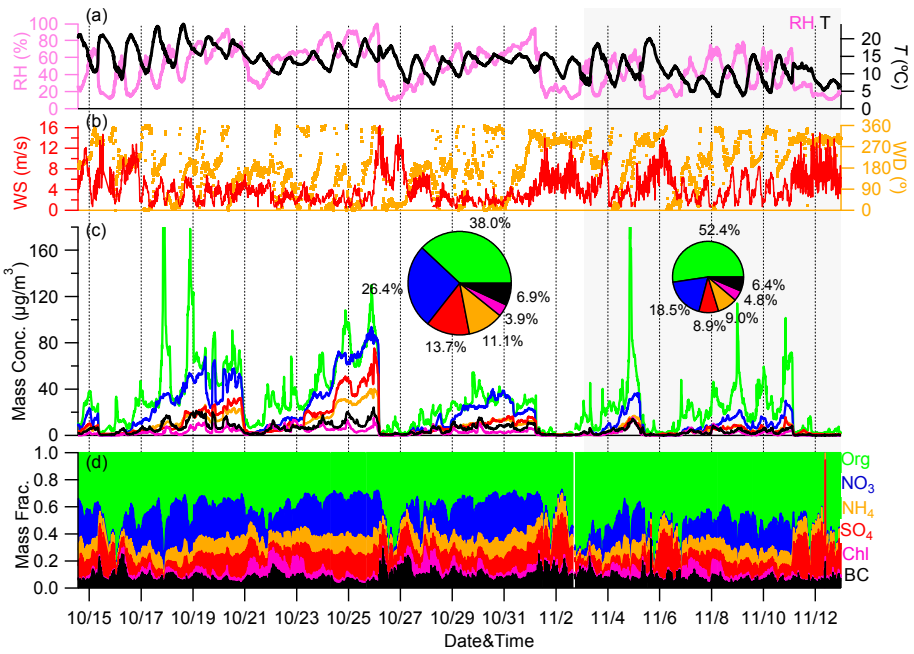

Figure~~Fig.~~ 1. Time series of (a) relative humidity (RH), temperature (*T*), (b) wind direction (WD), wind speed (WS), (c) mass concentrations, and (d) mass fractions of chemical species in PM_1. The pie charts show the average chemical composition of PM_1 measured before and during the Asia–Pacific Economic Cooperation (APEC) summit.

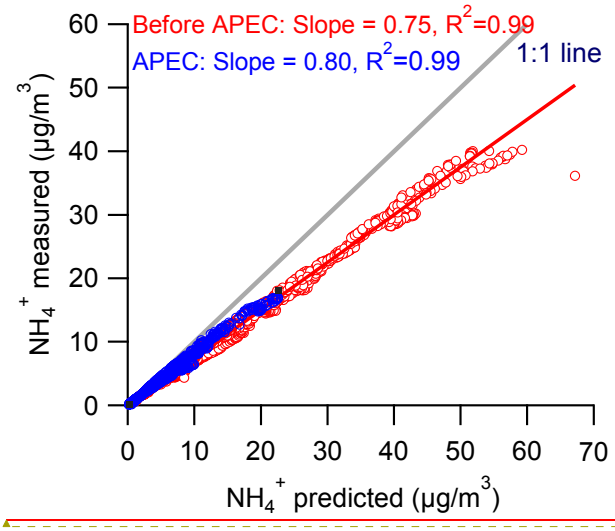

~~**Fig. 2.** Correlation between predicted NH_4^+ and measured NH_4^+ recorded before and during the Asia–Pacific Economic Cooperation (APEC) summit.~~

Formatted: Font: (Asian) +Body Asian, 12 pt

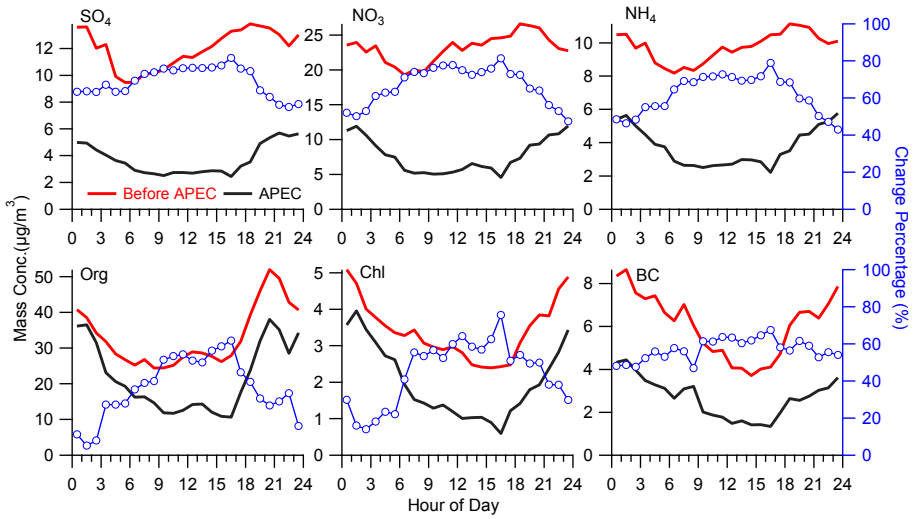

Figure~~Fig. 3~~2. Diurnal profiles of the mass concentrations of PM_1 species measured before and during the Asia–Pacific Economic Cooperation (APEC) summit. Also shown are the changes in percentage of aerosol species occurring during APEC.

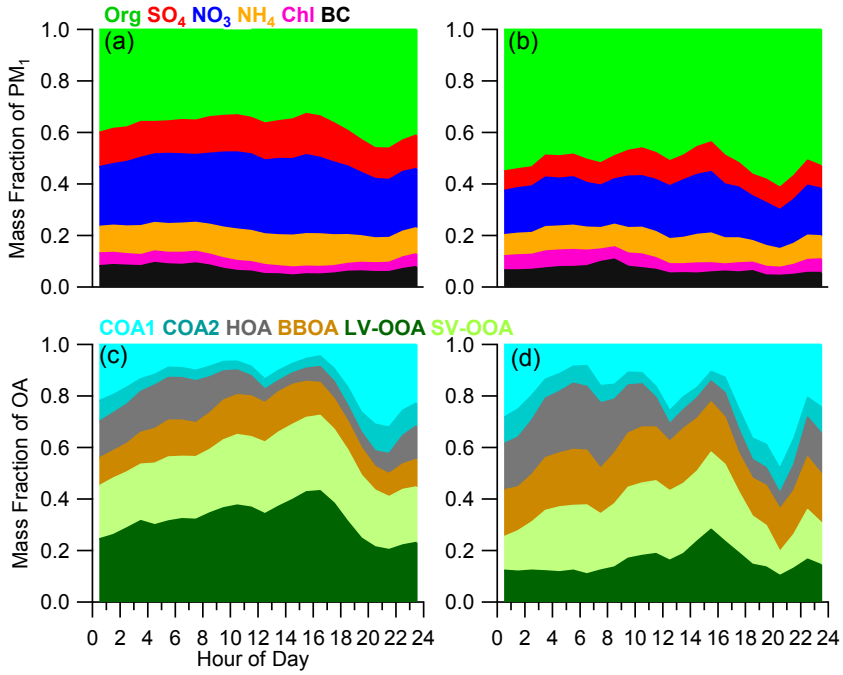

~~**Fig. 4.** Diurnal evolution of the composition of PM_1 and organic aerosols (OA) measured (a), (c) before the Asia–Pacific Economic Cooperation summit (APEC) and (b), (d) during APEC.~~

Formatted: Font: (Asian) +Body Asian, 12 pt, Bold, Font color: Accent 2

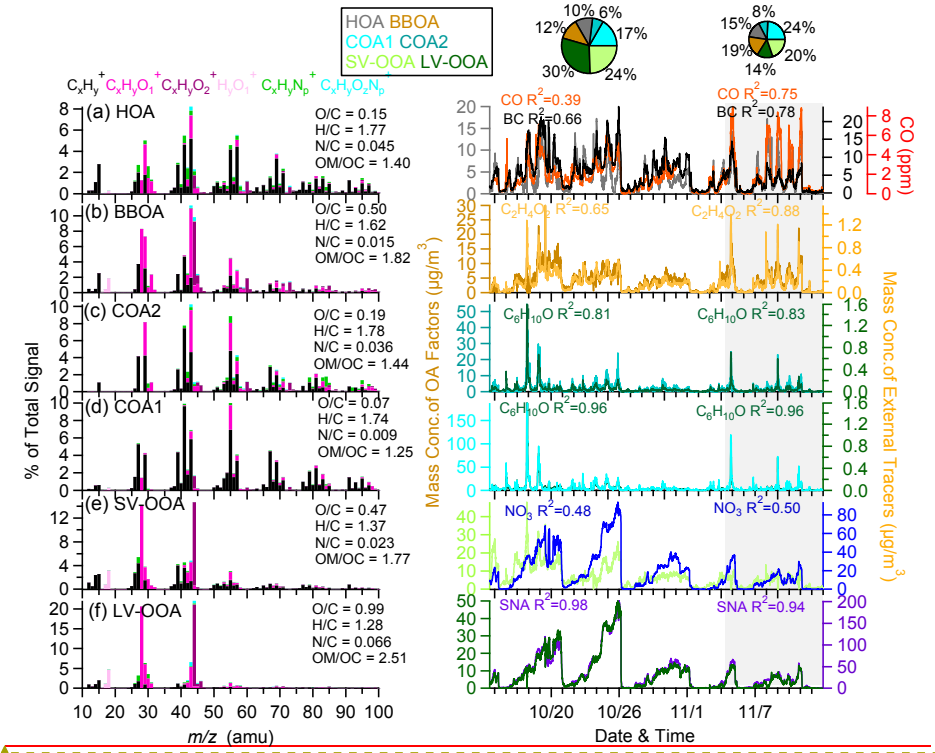

Formatted: Font: (Asian) +Body Asian, 12 pt

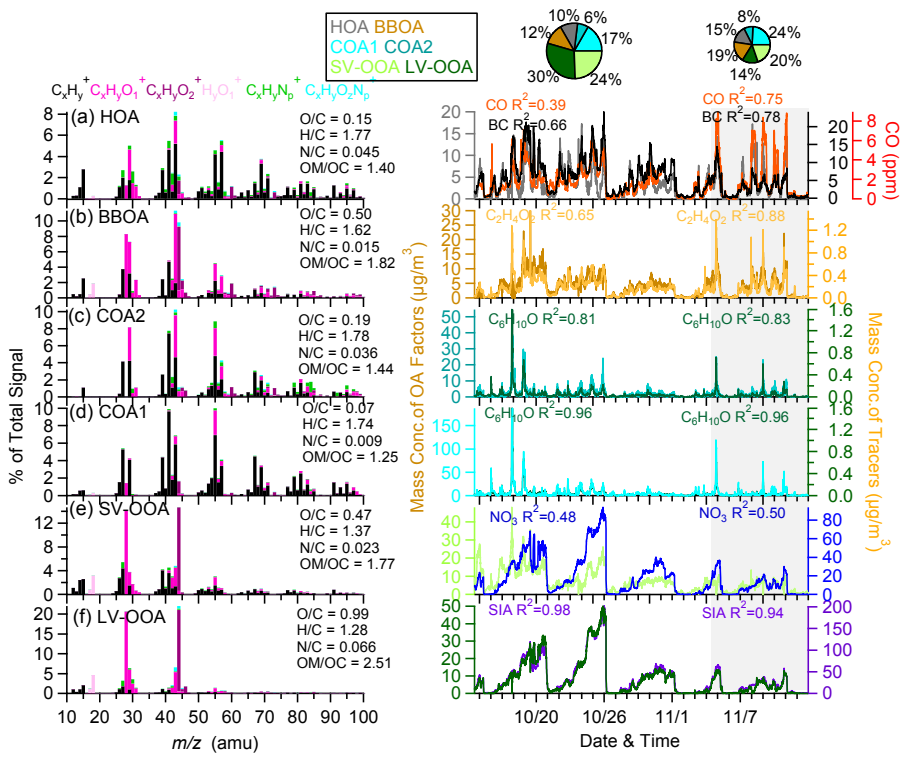

Figure~~Fig.~~ 53. High-resolution mass spectra (HRMS; left panel) and time series (right panel) of six organic aerosols (OA) components (a) hydrocarbon-like aerosol (HOA), (b) biomass burning OA (BBOA), (c) cooking organic aerosol 2 (COA2), (d) COA1, (e) semi-volatile oxygenated OA (SV-OOA), and (f) low-volatility oxygenated OA (LV-OOA). Also shown in the right panel are the time series of ~~external~~ tracers including $C_6H_{10}O^+$, $C_2H_4O_2^+$, CO, black carbon (BC), nitrate and ~~SNA~~ SIA (sulfate + nitrate + ammonium). The two pie charts show the average chemical composition of PM_1 measured before and during the Asia–Pacific Economic Cooperation (APEC) summit, respectively. The correlation coefficients between OA factors and external tracers measured before and during APEC are also shown in the figure.

Formatted: Font: (Asian) +Body Asian, 12 pt

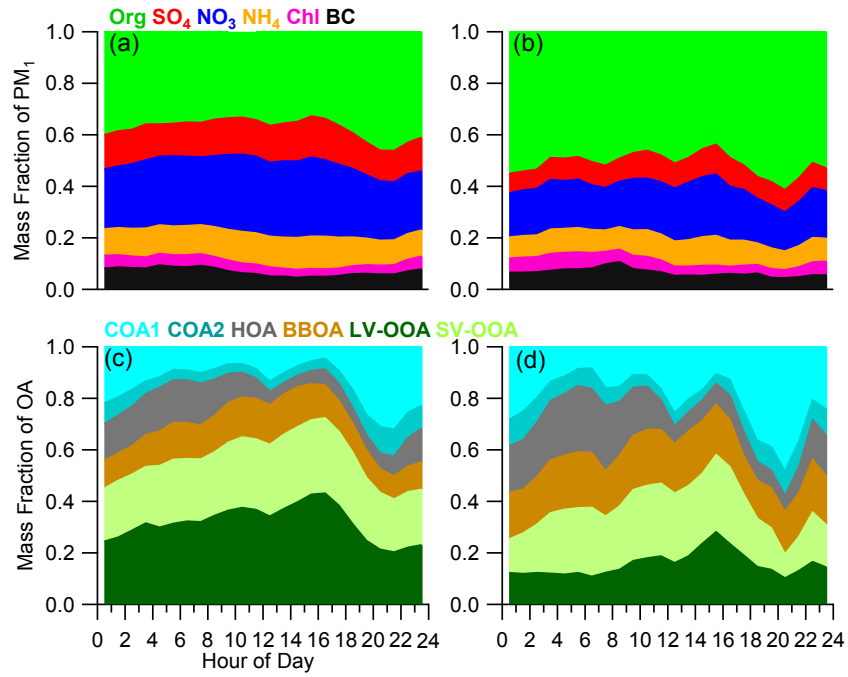

Figure 4. Diurnal evolution of the composition of PM_1 and organic aerosols (OA) measured (a), (c) before the Asia–Pacific Economic Cooperation summit (APEC) and (b), (d) during APEC.

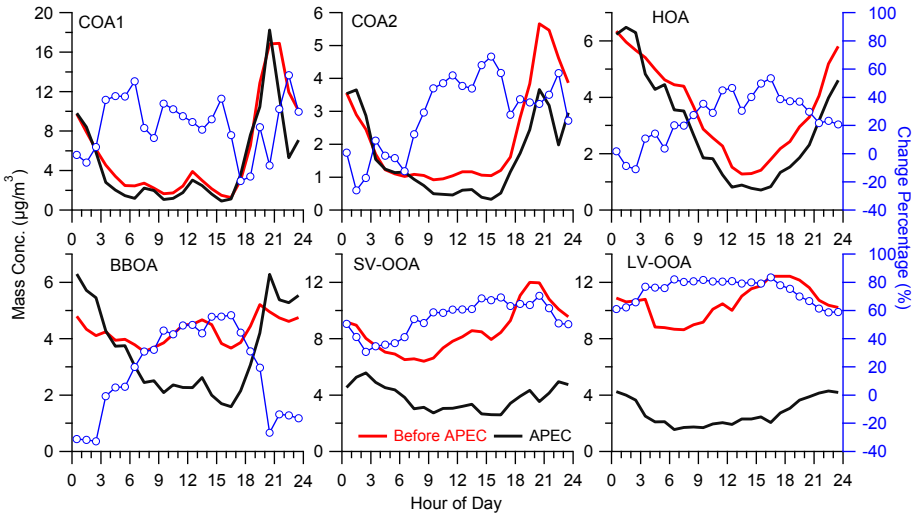

Figure~~Fig.~~ 65. Diurnal profiles of the mass concentrations of organic aerosol (OA) factors measured before and during the Asia–Pacific Economic Cooperation (APEC)

Formatted: Font: (Asian) +Body Asian, 12 pt, Bold, Font color: Accent 2

summit. Also shown are the changes in percentage of OA factors measured during APEC.

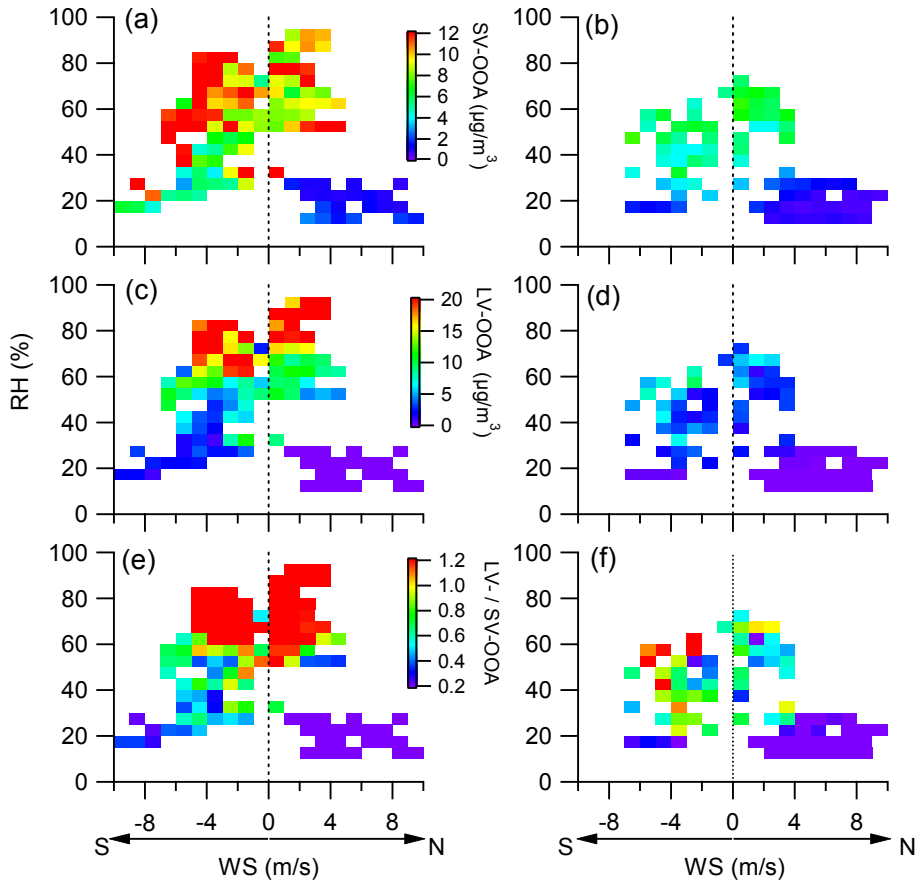

Figure~~Fig. 7~~6. Relative humidity (RH) and wind dependence (WD) of (a), (b) semi-volatile oxygenated organic aerosols (SV-OOA), (c), (d) low-volatility oxygenated organic aerosols (LV-OOA), and (e), (f) the ratio of LV-OOA/SV-OOA measured before (left panel) and during the Asia–Pacific Economic Cooperation (APEC) summit (right panel). S refers to the south (90° < WD < 270°), and N refers to the north (0°< WD < 90° and 270° < WD < 360°). Grids with points numbering less than five were excluded.

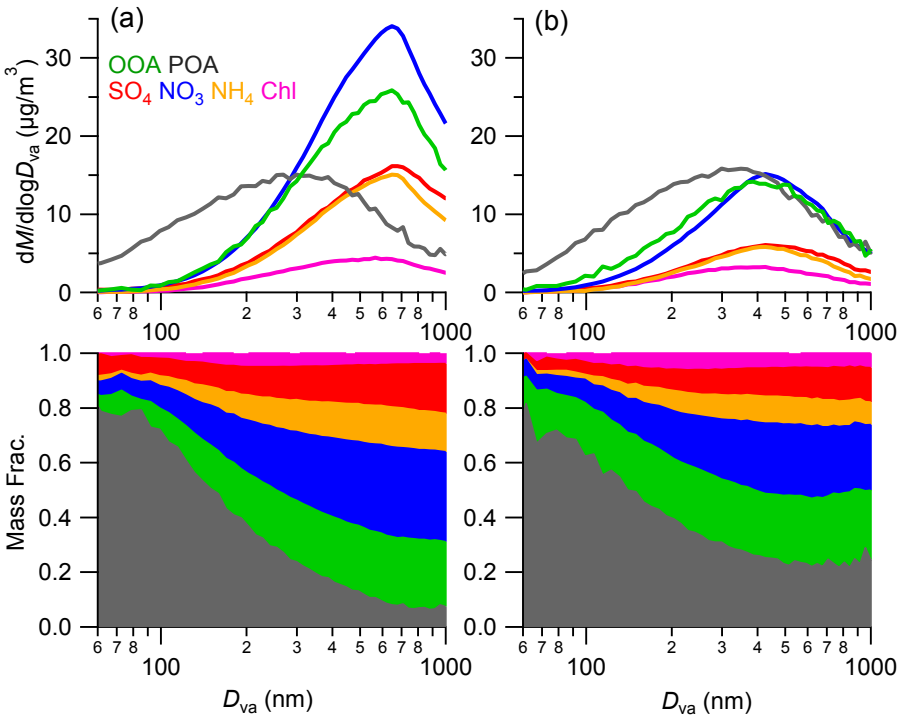

Figure~~Fig. 8~~7. Average size distributions and fractions of NR-PM_1 species, primary organic aerosols (POA) and oxygenated organic aerosols (OOA) measured (a) before the Asia–Pacific Economic Cooperation (APEC) summit and (b) during APEC.

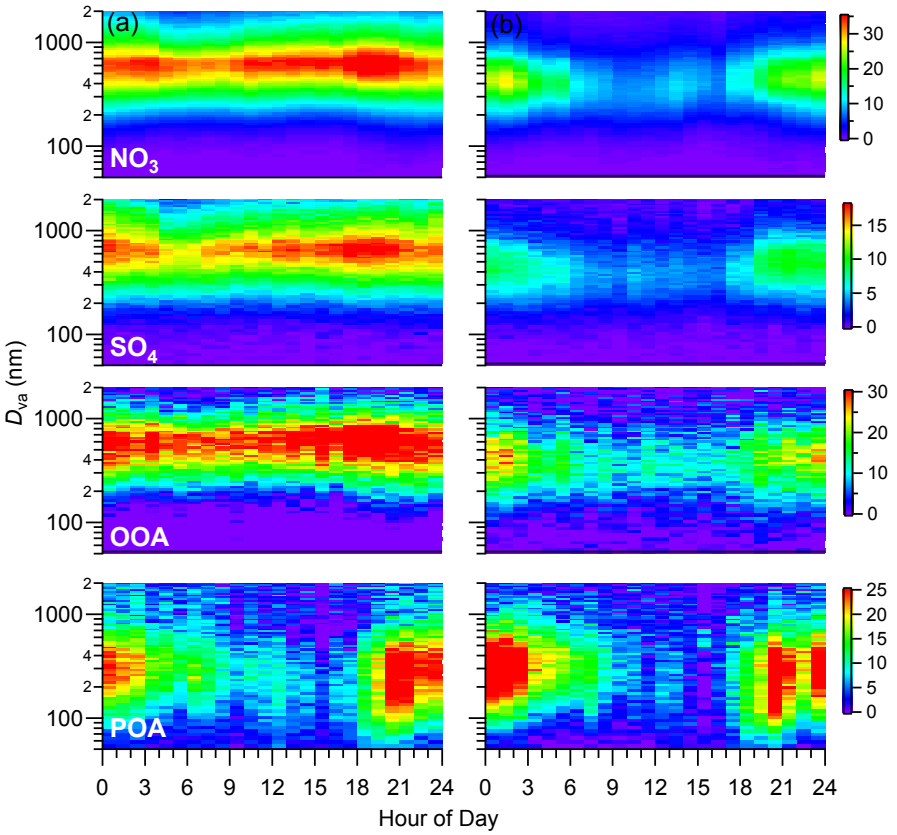

Figure~~Fig.~~ ~~98~~. Diurnal evolution of the size distributions of NR-PM_1 species measured (a) before the Asia–Pacific Economic Cooperation (APEC) and (b) during APEC.

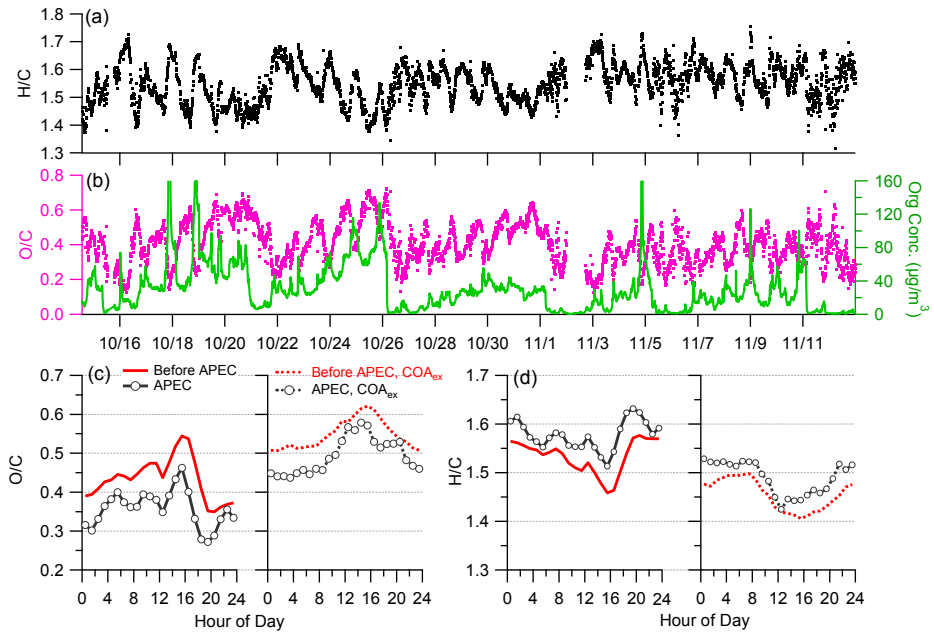

Figure~~Fig.~~ ~~10~~9. Time series of (a) H/C, (b) O/C, and organics, and diurnal variations of (c) O/C and (d) H/C. The dashed lines in (c) and (d) indicate the elemental ratios by excluding the contributions from cooking aerosols.

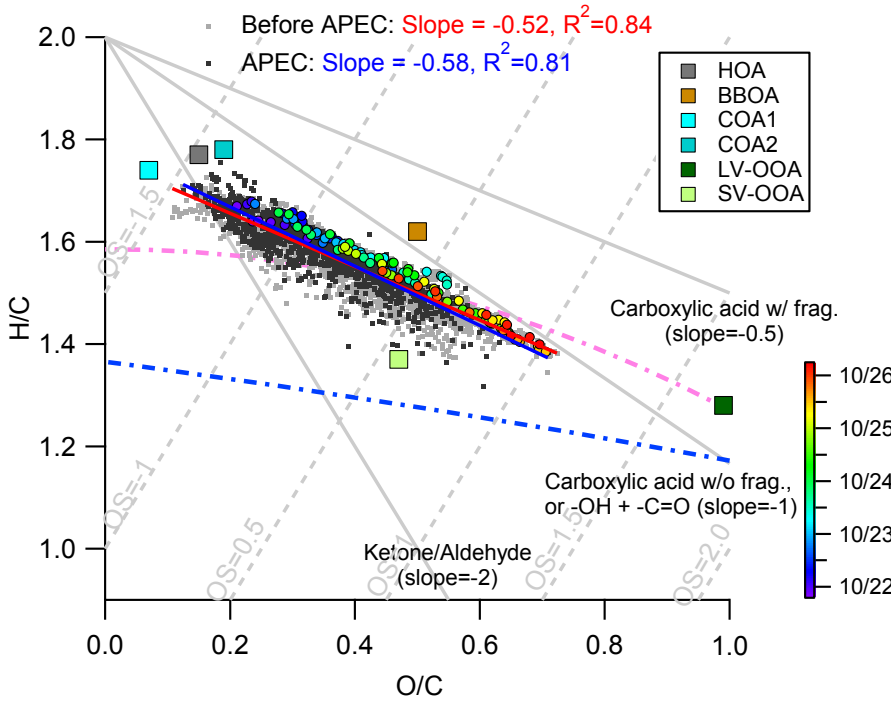

Figure ~~Fig.11~~10. Van Krevelen diagram of H/C versus O/C. The dashed lines indicate changes in H/C against O/C due to the addition of specific functional groups to aliphatic carbon (Heald et al., 2010). The pink and blue lines are derived from the right and left lines in the triangle plot of positive matrix factors (PMF) determined from 43 sites in the Northern Hemisphere (Ng et al., 2011). The color-coded H/C versus O/C refers to the data measured during the severe haze episode shown in Fig. ~~13~~12.

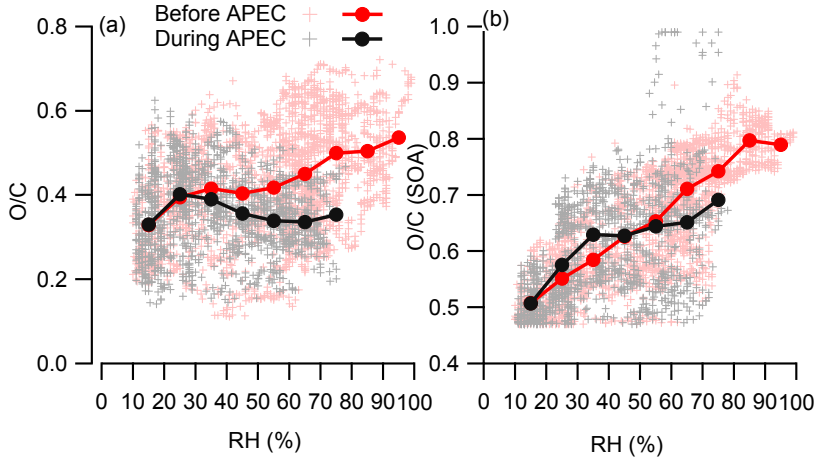

Figure~~Fig.~~ ~~12~~11. Variations in (a) O/C and (b) O/C of secondary organic aerosols (SOA) as a function of relative humidity (RH) measured (a) before the Asia–Pacific Economic Cooperation (APEC) summit and (b) during APEC. The data are also binned according to RH with increments of 10%.

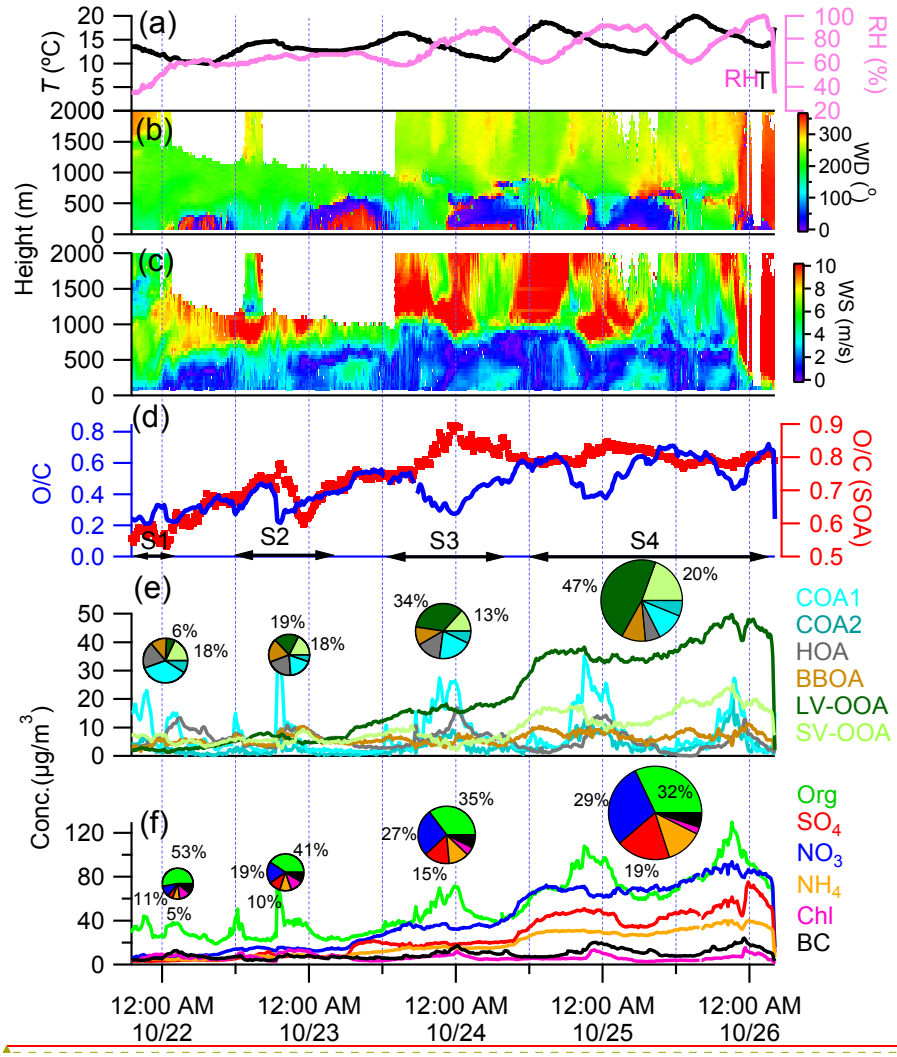

Formatted: Font: (Asian) +Body Asian, 12 pt, Bold

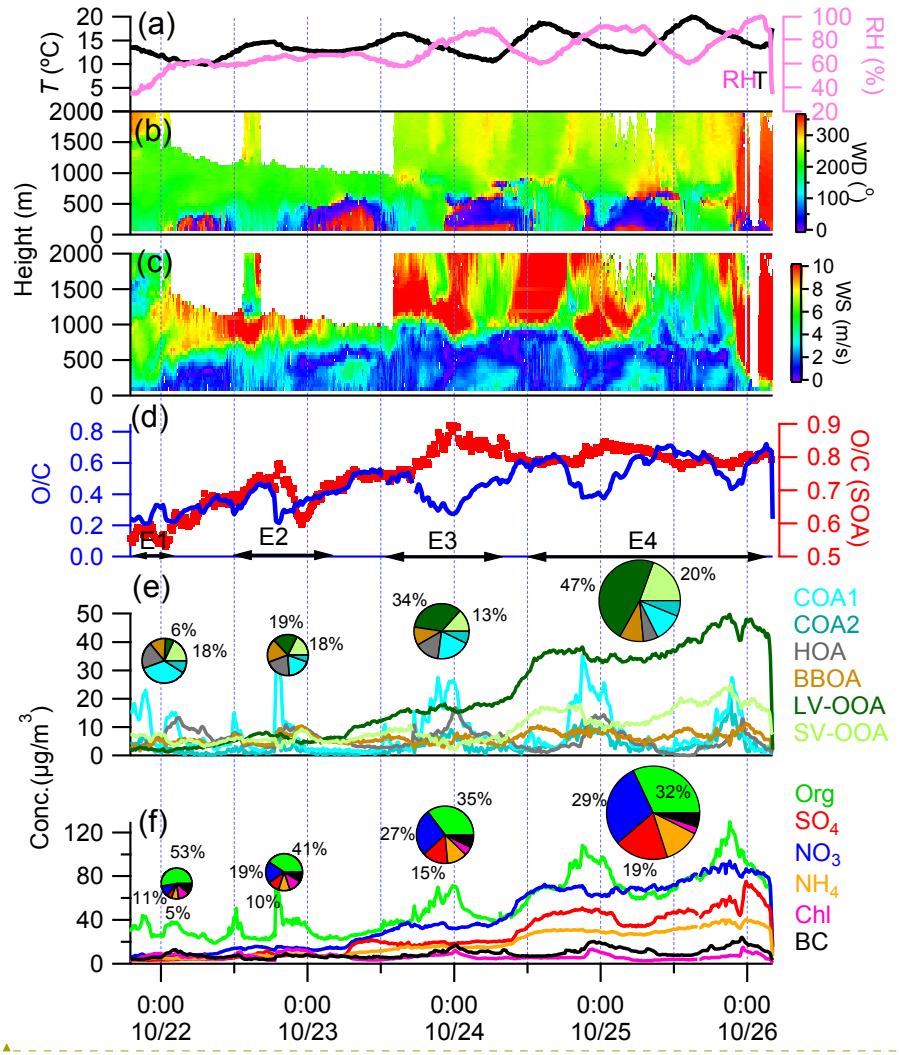

Figure ~~Fig. 13~~12. Evolution of meteorological variables including (a)–(c) relative humidity (RH), temperature (*T*), and vertical profiles of wind direction (WD) and wind speed (WS); (d) O/C and O/C of secondary organic aerosols (SOA); (e) organic aerosol (OA) factors; and (f) PM_1 species. The pie charts show the average chemical composition of PM_1 and OA for each stage. The numbers on the pie charts show the contributions of (e) semi-volatile oxygenated organic aerosols (SV-OOA) and low-volatility oxygenated organic aerosols (LV-OOA) and (f) organics, nitrate, and sulfate.

Formatted: Font: (Asian) +Body Asian, 12 pt, Bold

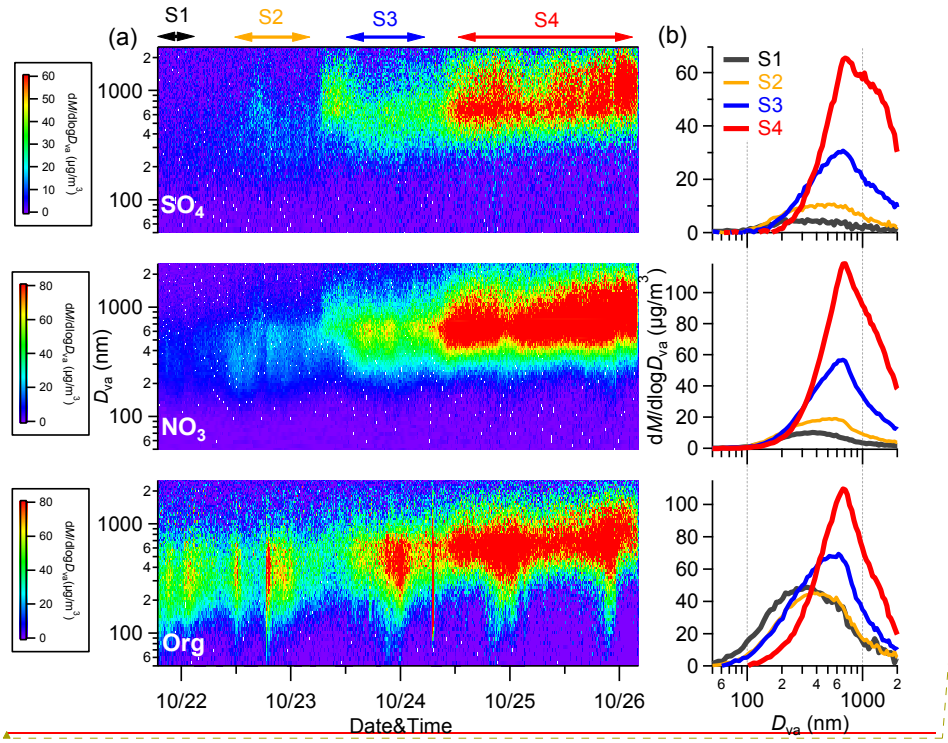

1190

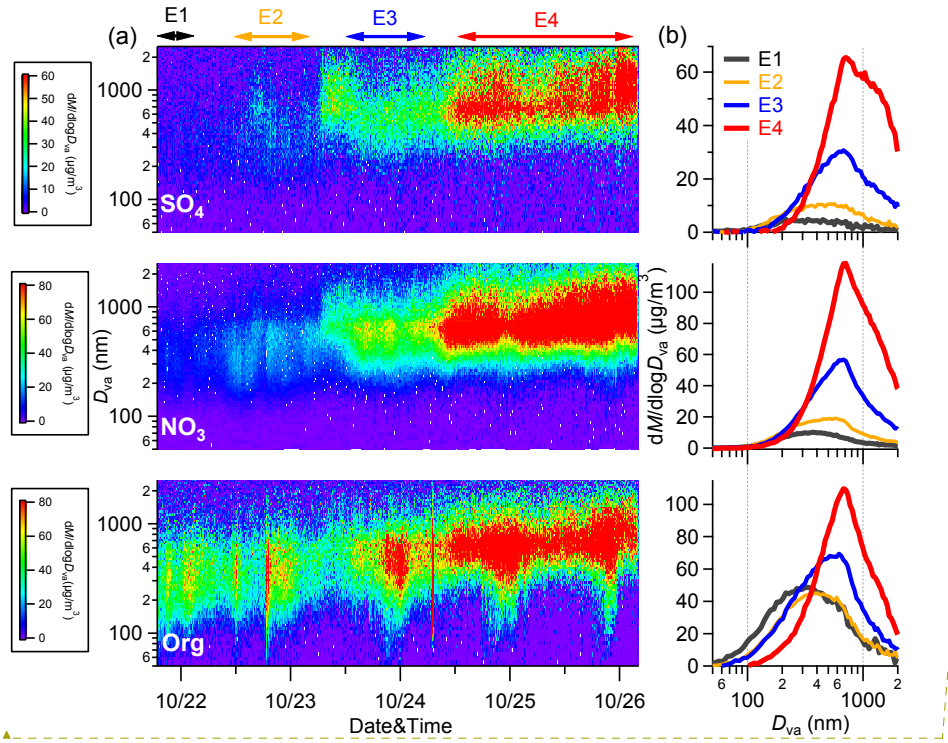

1191

Formatted: Font: (Asian) +Body Asian

Formatted: Font: (Asian) +Body Asian

Figure~~Fig. 14~~13. (a) Evolution of size distributions of sulfate, nitrate, and organics during the severe haze episode between October 22 and 25 (Fig.12). (b) Average size distributions of sulfate, nitrate, and organics during the four stages of E1-E4.~~these three species for each stage~~.